

# *Current and emerging developments in subseasonal to decadal prediction*

Article

Accepted Version

Merryfield, W. J., Baehr, J., Batte, L., Becker, E. J., Butler, A. H., Coelho, C. A., Danabasoglu, G., Dirmeyer, P. A., Doblaser-Reyes, F. J., Domeisen, D. I., Ferranti, L., Ilynia, T., Kumar, A., Muller, W. A., Rixen, M., Robertson, A. W., Smith, D. M., Takaya, Y., Tuma, M., Vitart, F., White, C. J., Alvarez, M. S., Ardilouze, C., Attard, H., Baggett, C., Balmaseda, M. A., Beraki, A. F., Battacharjee, P. S., Bilbao, R., Marques De Andrade, F., DeFlorio, M. J., Diaz, L. B., Ehsan, M. A., Frangkoulidis, G., Grainger, S., Green, B. W., Hell, M. C., Infanti, J. M., Isensee, K., Kataoka, T., Kirtman, B. P., Klingaman, N. P. ORCID: <https://orcid.org/0000-0002-2927-9303>, Lee, J.-Y., Mayer, K., McKay, R., Mecking, J., Miller, D. E., Neddermann, N., Ng, C. H., Osso, A., Pankatz, K., Peatman, S., Pegion, K., Perwitz, J., Raclade-Coronel, G. C., Reintges, A., Renkl, C., Solaraju-Murali, B., Spring, A., Stan, C., Sun, Y. Q., Tozer, C. R., Vigaud, N., Woolnough, S. ORCID: <https://orcid.org/0000-0003-0500-8514> and Yeager, S. (2020) Current and emerging developments in subseasonal to decadal prediction. *Bulletin of the American Meteorological Society*, 101 (6). E869-E896. ISSN 1520-0477 doi: <https://doi.org/10.1175/BAMS-D-19-0037.1> Available at <https://centaur.reading.ac.uk/88780/>

It is advisable to refer to the publisher's version if you intend to cite from the work. See [Guidance on citing](#).

To link to this article DOI: <http://dx.doi.org/10.1175/BAMS-D-19-0037.1>

Publisher: American Meteorological Society

All outputs in CentAUR are protected by Intellectual Property Rights law, including copyright law. Copyright and IPR is retained by the creators or other copyright holders. Terms and conditions for use of this material are defined in the [End User Agreement](#).

[www.reading.ac.uk/centaur](http://www.reading.ac.uk/centaur)

## **CentAUR**

Central Archive at the University of Reading

Reading's research outputs online

1 **Current and emerging developments in subseasonal to decadal prediction**

2  
3 William J. Merryfield

4 *Canadian Centre for Climate Modelling and Analysis, Environment and Climate Change Canada,*  
5 *Victoria, Canada*

6  
7 Johanna Baehr

8 *Institute of Oceanography, University of Hamburg, Hamburg, Germany*

9  
10 Lauriane Batté

11 *CNRM, Université de Toulouse, Météo France, CNRS, Toulouse, France*

12  
13 Emily J. Becker

14 *NOAA/NWS/NCEP/Climate Prediction Center/Innovim, LLC, College Park, Maryland*

15  
16 Amy H. Butler

17 *CIRES, University of Colorado Boulder, and Chemical Sciences Division, NOAA/ESRL, Boulder,*  
18 *Colorado*

19  
20 Caio A. S. Coelho

21 *CPTEC/INPE Center for Weather Forecasts and Climate Studies, Cachoeira Paulista, Brazil*

22  
23 Gokhan Danabasoglu

24 *Climate and Global Dynamics Laboratory, NCAR, Boulder, Colorado*

25  
26 Paul A. Dirmeyer

27 *Center for Ocean–Land–Atmosphere Studies, George Mason University, Fairfax, Virginia*

28  
29 Francisco J. Doblas-Reyes

30 *Barcelona Supercomputing Center and ICREA, Barcelona, Spain*

31  
32 Daniela I. V. Domeisen

33 *Institute for Atmospheric and Climate Science, ETH Zürich, Zurich, Switzerland*

34  
35 Laura Ferranti

36 *ECMWF, Reading, United Kingdom*

37  
38 Tatiana Ilynia

39 *Max Planck Institute for Meteorology, Hamburg, Germany*

40  
41 Arun Kumar

42 *Climate Prediction Center, NOAA/NWS/NCEP, College Park, Maryland*

44 Wolfgang A. Müller  
45 *Max Planck Institute for Meteorology and Deutscher Wetterdienst, Hamburg, Germany*  
46  
47 Michel Rixen  
48 *World Climate Research Programme, World Meteorological Organization, Geneva, Switzerland*  
49  
50 Andrew W. Robertson  
51 *International Research Institute for Climate and Society (IRI), Columbia University, Palisades, NY*  
52  
53 Doug M. Smith  
54 *Met Office Hadley Centre, Met Office, Exeter, UK*  
55  
56 Yuhei Takaya  
57 *Department of Atmosphere, Ocean and Earth System Modeling Research, Meteorological*  
58 *Research Institute, Japan Meteorological Agency, Tsukuba, Japan*  
59  
60 Matthias Tuma  
61 *World Climate Research Programme, World Meteorological Organization, Geneva, Switzerland*  
62  
63 Frederic Vitart  
64 *ECMWF, Reading, United Kingdom*  
65  
66 Christopher J. White  
67 *Department of Civil and Environmental Engineering, University of Strathclyde, Glasgow, United*  
68 *Kingdom*  
69  
70 Mariano S. Alvarez  
71 *Universidad de Buenos Aires, Centro de Investigaciones del Mar y la Atmósfera, Institut Franco-*  
72 *Argentin d'Estudes sur le Climat et ses Impacts, Buenos Aires, Argentina*  
73  
74 Constantin Ardilouze  
75 *CNRM, Université de Toulouse, Météo France, CNRS, Toulouse, France*  
76  
77 Hannah Attard  
78 *Embry-Riddle Aeronautical University-Worldwide, Daytona Beach, Florida*  
79  
80 Cory Baggett  
81 *Department of Atmospheric Science, Colorado State University, Fort Collins, Colorado, and*  
82 *NOAA/NWS/NCEP/Climate Prediction Center/Innovim, LLC, College Park, Maryland*  
83  
84 Magdalena A. Balmaseda  
85 *ECMWF, Reading, United Kingdom*  
86  
87 Asmerom F. Beraki

88 *CSIR – Global Change, Climate and Air Quality Modelling, and Department of Geography,*  
89 *Geoinformatics and Meteorology, University of Pretoria, Pretoria, South Africa*  
90  
91 Partha S. Bhattacharjee  
92 *I.M. Systems Group, NOAA/NWS National Centers for Environmental Prediction, College Park,*  
93 *Maryland*  
94  
95 Roberto Bilbao  
96 *Barcelona Supercomputing Center, Barcelona, Spain*  
97  
98 Felipe M. de Andrade  
99 *National Centre for Atmospheric Science, Department of Meteorology, University of Reading,*  
100 *Reading, United Kingdom*  
101  
102 Michael J. DeFlorio  
103 *Center for Western Weather and Water Extremes, Scripps Institution of Oceanography,*  
104 *University of California, San Diego, California*  
105  
106 Leandro B. Díaz  
107 *Universidad de Buenos Aires, Centro de Investigaciones del Mar y la Atmósfera, Institut Franco-*  
108 *Argentin d’Estudes sur le Climat et ses Impacts, Buenos Aires, Argentina*  
109  
110 Muhammad Azhar Ehsan  
111 *Earth System Physics Section, International Centre for Theoretical Physics, Trieste, Italy, and*  
112 *Center of Excellence for Climate Change Research, King Abdulaziz University, Jeddah, Saudi*  
113 *Arabia*  
114  
115 Georgios Fragkoulidis  
116 *Institute for Atmospheric Physics, Johannes Gutenberg University, Mainz, Germany*  
117  
118 Sam Grainger  
119 *Sustainability Research Institute, School of Earth and Environment, University of Leeds, Leeds,*  
120 *United Kingdom*  
121  
122 Benjamin W. Green  
123 *Cooperative Institute for Research in Environmental Sciences, University of Colorado, and*  
124 *NOAA/OAR/ESRL/Global Systems Division, Boulder, Colorado*  
125  
126 Momme C. Hell  
127 *Scripps Institution of Oceanography, La Jolla, California*  
128  
129 Johnna M. Infanti  
130 *Cherokee Nation Strategic Programs, and NOAA/Office of Oceanic and Atmospheric*  
131 *Research/Office of Weather and Air Quality, Silver Spring, Maryland*

132  
133 Katharina Isensee  
134 *Deutscher Wetterdienst, Offenbach, Germany*  
135  
136 Takahito Kataoka  
137 *Japan Agency for Marine-Earth Science and Technology, Kanagawa, Japan*  
138  
139 Ben P. Kirtman  
140 *University of Miami, Rosenstiel School for Marine and Atmospheric Sciences, Miami, Florida*  
141  
142 Nicholas P. Klingaman  
143 *National Centre for Atmospheric Science, Department of Meteorology, University of Reading,*  
144 *Reading, United Kingdom*  
145  
146 June-Yi Lee  
147 *Research Center for Climate Sciences, Pusan National University and Center for Climate Physics,*  
148 *Institute for Basic Science, Busan, Korea*  
149  
150 Kirsten Mayer  
151 *Department of Atmospheric Science, Colorado State University, Fort Collins, Colorado*  
152  
153 Roseanna McKay,  
154 *School of Earth, Atmosphere and Environment, Monash University, Melbourne, Australia*  
155  
156 Jennifer V Mecking  
157 *Ocean and Earth Science, University of Southampton, Southampton, United Kingdom*  
158  
159 Douglas E. Miller  
160 *University of Illinois at Urbana–Champaign, Urbana, Illinois*  
161  
162 Nele Neddermann  
163 *Institute for Oceanography, CEN, Universität Hamburg, and International Max Planck Research*  
164 *School on Earth System Modelling, Max Planck Institute for Meteorology, Hamburg, Germany*  
165  
166 Ching Ho Justin Ng  
167 *Atmospheric and Oceanic Sciences (AOS), Princeton University, Princeton, New Jersey*  
168  
169 Albert Ossó  
170 *NCAS-Climate, University of Reading, Reading, United Kingdom*  
171  
172 Klaus Pankatz  
173 *Deutscher Wetterdienst, Offenbach, Germany and Max Planck Institut für Meteorologie,*  
174 *Hamburg, Germany*  
175

176 Simon Peatman  
177 *School of Earth and Environment, University of Leeds, Leeds, United Kingdom*  
178  
179 Kathy Pegion  
180 *George Mason University, Fairfax, Virginia*  
181  
182 Judith Perlwitz  
183 *CIRES, University of Colorado Boulder, and Physical Sciences Division, NOAA/ESRL, Boulder,*  
184 *Colorado*  
185  
186 G. Cristina Recalde-Coronel  
187 *Department of Earth and Planetary Sciences, Johns Hopkins University, Baltimore, Maryland,*  
188 *and Facultad de Ingeniería Marítima y Ciencias del Mar, Escuela Superior Politécnica del Litoral,*  
189 *Guayaquil, Ecuador*  
190  
191 Annika Reintges  
192 *GEOMAR Helmholtz Centre for Ocean Research, Kiel, Germany*  
193  
194 Christoph Renkl  
195 *Department of Oceanography, Dalhousie University, Halifax, Canada*  
196  
197 Balakrishnan Solaraju-Murali  
198 *Barcelona Supercomputing Center, Barcelona, Spain*  
199  
200 Aaron Spring  
201 *Max Planck Institute for Meteorology, Hamburg, Germany*  
202  
203 Cristiana Stan  
204 *Department of Atmospheric, Oceanic and Earth Sciences, George Mason University, Fairfax,*  
205 *Virginia*  
206  
207 Y. Qiang Sun  
208 *Atmospheric and Oceanic Sciences Program, Princeton University, Princeton, New Jersey*  
209  
210 Carly R. Tozer  
211 *CSIRO Oceans and Atmosphere, Hobart, Tasmania, Australia*  
212  
213 Nicolas Vigaud  
214 *International Research Institute for Climate and Society (IRI), Columbia University, Palisades, NY*  
215  
216 Steven Woolnough  
217 *National Centre for Atmospheric Science, University of Reading, Reading, UK*  
218  
219 Stephen Yeager

220 *National Center for Atmospheric Research, Boulder, Colorado, USA*

221

222

223

224

225 Corresponding author: William Merryfield ([bill.merryfield@canada.ca](mailto:bill.merryfield@canada.ca))

226

227

228

229

230

231 **Abstract**

232 Weather and climate variations on subseasonal to decadal timescales can have enormous

233 social, economic and environmental impacts, making skillful predictions on these timescales a

234 valuable tool for decision makers. As such, there is a growing interest in the scientific,

235 operational, and applications communities in developing forecasts to improve our

236 foreknowledge of extreme events. On subseasonal to seasonal (S2S) timescales, these include

237 high-impact meteorological events such as tropical cyclones, extratropical storms, floods,

238 droughts, and heat and cold waves. On seasonal to decadal (S2D) timescales, while the focus

239 broadly remains similar, (e.g., on precipitation, surface and upper ocean temperatures and their

240 effects on the probabilities of high-impact meteorological events), understanding the roles of

241 internal and externally-forced variability such as anthropogenic warming in forecasts also

242 becomes important.

243

244 The S2S and S2D communities share common scientific and technical challenges. These include

245 forecast initialization and ensemble generation; initialization shock and drift; understanding the

246 onset of model systematic errors; bias correction, calibration, and forecast quality assessment;

247 model resolution; atmosphere-ocean coupling; sources and expectations for predictability; and



248 linking research, operational forecasting, and end user needs. In September 2018 a coordinated  
249 pair of international conferences, framed by the above challenges, was organized jointly by the  
250 World Climate Research Programme (WCRP) and the World Weather Research Programme  
251 (WWRP). These conferences surveyed the state of S2S and S2D prediction, ongoing research,  
252 and future needs, providing an ideal basis for synthesizing current and emerging developments  
253 in these areas that promise to enhance future operational services. This article provides such a  
254 synthesis.

255

#### 256 **Capsule**

257 Climate prediction on subseasonal to decadal time scales is a rapidly advancing field that is  
258 synthesizing improvements in climate process understanding and modeling to improve and  
259 expand operational services worldwide.

260

261

262

263

264

265

266

267

268

269

270 **[Introductory text]**

271 Beyond the tremendous progress in weather forecasting witnessed in recent decades (Bauer et  
272 al. 2015), predictive capabilities have expanded, increasingly seamlessly, to encompass climate  
273 on subseasonal to decadal time scales (Fig. 1 and Kirtman et al. 2013). These advances have  
274 been enabled by better observations, data assimilation schemes, and models originating both  
275 from the weather prediction and long term climate simulation communities, together with  
276 increased computational power supporting progressively higher resolution and larger  
277 ensembles that allow uncertainties to be better estimated and in some cases reduced.

278  
279 International efforts under the auspices of the World Weather Research Programme (WWRP)  
280 and World Climate Research Programme (WCRP) have helped drive this progress through  
281 coordinated research to improve the accuracy and utilization of weather and climate  
282 predictions. Community research efforts under the WCRP led initially to climate predictions one  
283 to two seasons ahead becoming part of the World Meteorological Organization (WMO)  
284 operational infrastructure (Graham et al. 2011). More recently a joint WWRP and WCRP  
285 Subseasonal to Seasonal Prediction Project has started tackling the so-called weather-climate  
286 prediction desert from two weeks to a season (Robertson et al. 2018; Mariotti et al. 2018),  
287 aiming to underpin new WMO operations on those time scales (Vitart et al. 2017), and the  
288 NOAA-led SubX project has similar aims (Pegion et al. 2019). At longer ranges, WCRP-enabled  
289 research has quantified predictability from a year to a decade, and corresponding WMO  
290 operational infrastructure for annual-to-decadal climate prediction is now in place (World  
291 Meteorological Organization 2018; Kushnir et al. 2019).

292

293 As each of these efforts has progressed it has become increasingly apparent that common  
294 challenges exist across predictive time scales. These include understanding and adequately  
295 representing in models processes that give rise to predictability in the Earth system, consisting  
296 of the physical climate system—atmosphere, ocean, land and sea ice—together with associated  
297 biogeochemical cycling, especially of carbon (upper part of Fig. 1); capturing and  
298 communicating inherent uncertainties caused by the chaotic nature of weather and climate;  
299 correcting for and reducing imperfections in models that may systematically degrade forecast  
300 quality; and providing forecast information in a form that is applicable to decision making. At  
301 the same time, opportunities for usefully predicting elements of the Earth system beyond long-  
302 term means of standard meteorological variables , including land, ocean and sea ice properties  
303 and risks of weather extremes, have come into focus. The ultimate collective endeavor is to  
304 improve the prediction of the spatial–temporal continuum connecting weather to climate  
305 through a coordinated, seamless and integrated Earth system approach for the benefit of  
306 society.

307

308 In September 2018, international conferences<sup>1</sup> on subseasonal to seasonal prediction (S2S,  
309 encompassing forecast ranges from two weeks to a season) and seasonal to decadal prediction (S2D,  
310 encompassing ranges longer than a season, up to a decade) together with cross-cutting plenary

---

<sup>1</sup> The Second International Conference on Subseasonal to Seasonal Prediction (S2S) and Second International Conference on Seasonal to Decadal Prediction (S2D) were held 17-21 September 2018 at NCAR facilities in Boulder Colorado. These coordinated meetings involved 347 participants, including 92 early career scientists, from 38 countries, with a total of 368 oral and poster presentations. Further information including a complete list of contributions can be found at <https://www.wcrp-climate.org/s2s-s2d-2018-home>.

311 sessions were convened jointly by WWRP and WCRP. This represented a confluence of research  
312 and operational climate prediction expertise and knowledge exchange across prediction time  
313 scales that was unprecedented in scope. Selected outcomes, organized by themes  
314 encompassing the challenges outlined above, are synthesized in this article.

315

### 316 **Mechanisms of predictability.**

#### 317 *Subseasonal to Seasonal*

318 A major source of S2S predictability is the organization of tropical convection by the Madden  
319 Julian Oscillation, or MJO (Woolnough, 2019), which is predicted skillfully by S2S project models  
320 up to 3-4 weeks ahead (Vitart 2017). The MJO has worldwide impacts that depend on its  
321 amplitude and phase, including modulation of tropical cyclone activity (Lee et al. 2018; Zhao et  
322 al. 2019) and extratropical phenomena such as the East Asian summer monsoon (Li et al. 2018).  
323 The associated tropical-extratropical teleconnections (Lin et al. 2019) impart S2S forecast skill  
324 for many of these extratropical phenomena including Euro-Atlantic weather regimes, position  
325 of the jet stream, atmospheric rivers (DeFlorio et al. 2019), and hail/tornado activity (Baggett et  
326 al. 2018). However, good representations of the basic state both in the tropics and extratropics,  
327 as well as tropical air-sea interactions and atmospheric convection (e.g., Yoo et al. 2015), are  
328 necessary for these teleconnections to be correctly simulated by general circulation models  
329 (Henderson et al. 2017).

330

331 S2S predictability also derives from the stratosphere through its relatively long time scales of  
332 variability<sup>2</sup> and lagged influences on the troposphere (Kidston et al. 2015). Interactions  
333 between the stratosphere and the troposphere from the tropics to the extratropics thus  
334 provide a promising source of S2S prediction skill (Butler et al. 2019). For example, in the winter  
335 Northern Hemisphere stratosphere the climatological westerly polar vortex exhibits extremes  
336 in variability, including sudden stratospheric warmings (SSWs) that are driven largely by Rossby  
337 waves from the troposphere. SSWs have lagged impacts on sea level pressure, surface  
338 temperature and precipitation, including pronounced tendencies for cold anomalies over  
339 northern Eurasia and warm anomalies over northeastern North America (e.g., Sigmond et al.  
340 2013). Initializing forecasts during extreme stratospheric events provides increases in prediction  
341 skill of surface climate in such regions up to 3-6 weeks later (Domeisen et al. 2019c). However,  
342 the predictability of specific extreme stratospheric events is limited, ranging from a few days to  
343 about two weeks (Fig. 2) for different SSWs (Karpechko 2018; Taguchi 2018, Domeisen et al.  
344 2019a), although models show evidence of under-confident forecasts in the stratosphere on  
345 S2S timescales (O'Reilly et al. 2019). Outstanding questions remain about the mechanisms of  
346 stratosphere-troposphere coupling processes, in particular on the causes, variability, and trends  
347 for the occurrence of SSW events (Ayarzaguena et al. 2018; Simpson et al. 2018) and why not  
348 all SSW events have similar downward effects (e.g., Garfinkel et al. 2013, Maycock & Hitchcock,  
349 2015). In addition, further research is needed to assess the degree to which prediction models  
350 capture both the stratospheric variability and coupling processes.

---

<sup>2</sup> Including the quasi-biennial oscillation (QBO) of the tropical stratosphere, whose influences span a range of time scales and are addressed in the "Time scale interactions" subsection.

351

352 Among atmosphere-surface influences, land-atmosphere interactions have their greatest  
353 impact on subseasonal time scales in forecasts where land is initialized (Dirmeyer et al. 2018a),  
354 but also can contribute skill on weather prediction and multi-month time scales (Dirmeyer and  
355 Halder 2016, 2017). The most broadly impactful land attribute is soil moisture (Koster et al.  
356 2004, 2016), but anomalies in soil temperature (Y. Zhang et al. 2019; Yang et al. 2019), snow  
357 cover (Jeong et al. 2012; Orsolini et al. 2013), and vegetation states (Williams et al. 2016) can all  
358 have significant impacts. A number of recent studies have focused on non-local impacts of land  
359 surface anomalies, showing for example that soil moisture anomalies can exert remote as well  
360 as local influences in boreal summer through driving of quasi-stationary Rossby waves and  
361 associated circulation anomalies (e.g., Teng et al. 2019; Wang et al. 2019). In addition, land  
362 surface and subsurface temperatures in spring may exert delayed downstream influences on  
363 precipitation (Xue et al. 2018), and evapotranspiration may remotely influence precipitation  
364 over land (Wei and Dirmeyer 2019).

365

366 Atmosphere-ocean interactions, fundamental for S2D predictability, can also be influential on  
367 S2S time scales. For example submonthly prediction skills for precipitation and temperature are  
368 enhanced over certain land areas including parts of Australia, the Maritime Continent and the  
369 contiguous United States when tropical sea surface temperature (SST) anomalies associated  
370 with El Niño Southern Oscillation (ENSO) are present (Hudson et al. 2011; Li and Robertson  
371 2015; DelSole et al. 2017). Extratropical SST anomalies also can impart S2S skill through  
372 teleconnections, as shown for example by McKinnon et al. (2016) who identified a SST anomaly

373 pattern in the mid-latitude North Pacific that tends to precede heat waves and rainfall deficits  
374 in the eastern United States by up to 50 days.

375  
376 Sea ice strongly influences surface fluxes and lower atmospheric temperatures particularly in the  
377 marginal ice zone, and provides a source of S2S predictability for polar and possibly midlatitude  
378 regions (Chevallier et al. 2019). This motivates the development of S2S forecasts for sea ice,  
379 which thus far have shown significant, albeit region-dependent skill for predicting intraseasonal  
380 Arctic sea ice variability (Liu et al. 2018, Zampieri et al. 2018).

381  
382 *Seasonal to decadal*

383 A primary general source of S2D atmospheric predictability is remote influences from a variety  
384 of teleconnections (e.g., Yuan et al. 2018; Ruprich-Robert et al. 2018; Beverley et al. 2019).  
385 Teleconnections associated with anomalous atmospheric circulation patterns arise from  
386 changes to the Walker circulation usually driven by anomalous zonal SST gradients (Cai et al.  
387 2019), and changes to the Hadley circulation usually driven by anomalous meridional SST  
388 gradients, especially interhemispheric differences (Kang et al. 2018). These influences impact  
389 tropical cyclones and rainfall, whereas anomalous upper level divergence due to tropical rainfall  
390 anomalies leads to Rossby waves that impact the extratropics (Scaife et al. 2017; O'Reilly et al.  
391 2018). Besides giving rise to atmosphere-ocean interactions that alter the atmospheric  
392 circulation, SST anomalies can induce low-level temperature and moisture anomalies that are  
393 advected elsewhere by climatological winds (Dunstone et al. 2018).

394

395 S2D atmospheric predictability arising from teleconnections requires that SST anomalies be  
396 predictable. On seasonal timescales, tropical SST anomalies are dominated by ENSO (Yang et al.  
397 2018), though there is some independent variability in the tropical Atlantic and Indian Oceans  
398 that also drives teleconnections (e.g., Nnamchi et al. 2015; Lim et al. 2016). The impacts of  
399 ENSO are sensitive to ENSO diversity (Capotondi et al. 2015), including the longitude at which  
400 maximum SST anomalies occur (Yeh et al. 2018; Patricola et al. 2018). ENSO SST anomalies are  
401 largely predictable out to a year particularly in winter and early spring (Barnston et al. 2017),  
402 whereas predictability may extend to two years for some La Niña events (Di Nezio et al. 2017),  
403 and to 1 ½ to two years for certain El Niño events (Luo et al. 2008).

404

405 Decadal SST variability occurs in both the Atlantic and Pacific oceans, often referred to as  
406 Atlantic Multidecadal Variability (AMV) and Pacific Decadal Variability (PDV), e.g. Kushnir et al.  
407 (2019). The causes of AMV are not fully understood, especially the relative roles of internal  
408 variability and external forcing from aerosols. However, AMV is modulated to some extent by  
409 the oceanic Atlantic Meridional Overturning Circulation (Yeager and Robson 2017), which  
410 together with the North Atlantic subpolar gyre is influenced by deep ocean density anomalies  
411 particularly in the Labrador Sea (Robson et al. 2016); these influences contribute to the  
412 especially high multi-year predictability in the North Atlantic (Buckley et al. 2019). AMV couples  
413 to the Hadley circulation, affecting hurricanes and Sahel rainfall as illustrated in Fig. 3 (Sheen et  
414 al. 2017), and can initiate atmospheric Rossby waves with remote influences including  
415 temperatures in parts of China (Monerie et al. 2018). AMV can influence PDV (Ruprich-Robert  
416 et al. 2017), and vice-versa. PDV may also be influenced by off-equatorial heat content



417 anomalies in the western Pacific Ocean (Meehl et al. 2016). Decadal variability of deep  
418 convection in the Southern Ocean influences temperatures in that region, potentially explaining  
419 recent increases in Antarctic sea ice (L. Zhang et al. 2019).

420

421 S2D atmospheric predictability also arises from longer time scale processes over land, mainly  
422 involving soil moisture (Chikamoto et al. 2017; Ardilouze et al. 2019) and vegetation (Weiss et  
423 al. 2014; Bellucci et al. 2015). These highlight the need for land surface initialization  
424 (Prodhomme et al. 2016a) and realistic vegetation models (Alessandri et al. 2017).

425

426 An additional source of S2D predictability is variations in radiative forcing, which provide  
427 significant skill on multi-year timescales (Smith et al. 2019). Much of this skill arises from  
428 changes in greenhouse gases, but anthropogenic aerosols may force decadal variations in AMV  
429 (Booth et al. 2012) and PDV (Smith et al. 2016; Takahashi and Watanabe 2016). Solar variability  
430 (Misios et al. 2019), and volcanic eruptions (Menegoz et al. 2018) including through their  
431 influence on ENSO (Khodri et al. 2017; Wang et al. 2018) and possibly AMV and the North  
432 Atlantic Oscillation (NAO; Swingedouw et al. 2017) affect climate on seasonal to decadal  
433 timescales and are potentially important sources of predictability. However, the relative roles  
434 of external radiative forcing and internal variability (W. Kim et al. 2018) continue to be  
435 explored.

436

437 *Time scale interactions*

438 The Quasi-biennial Oscillation (QBO) is a downward-propagating ~28-month oscillation of  
439 easterly and westerly zonal jets in the tropical stratosphere, driven by upward equatorial waves  
440 from the troposphere (e.g., Kim and Chun 2015). In addition to having high predictability and  
441 some teleconnected influence on winter surface climate (e.g., Scaife et al. 2014a), the QBO  
442 modulates the amplitude, persistence, and rate of propagation of the boreal wintertime MJO  
443 (Fig. 4) through its impact on tropical convection via changes in static stability near the  
444 tropopause (Yoo and Son 2016, Nishimoto and Yoden 2017). MJO amplitude is better predicted  
445 at longer leads during the easterly phase of the QBO (Marshall et al. 2017), likely as a result of  
446 longer persistence of the MJO rather than its greater initial amplitude (Lim et al. 2019).

447

448 The modulation of SSW probability of occurrence by tropical sources of variability, such as the  
449 QBO, ENSO, or MJO, may extend probabilistic predictability of stratospheric variability to a few  
450 months or longer if these relationships can be adequately captured by prediction models  
451 (Garfinkel & Schwartz 2017; Garfinkel et al. 2018; Domeisen et al. 2019a,b).

452

453 There is increasing evidence of additional interactions between various sources of S2S and S2D  
454 predictability across time scales. One example is that seasonal time scale variations in ENSO  
455 modulate the MJO (Chen et al. 2016) and its impact on the NAO (Lee et al. 2019) with  
456 consequent influences on weather over remote regions. Another is that ENSO teleconnection  
457 to the extratropics has varied over multi-decadal time scales spanning the past 100+ years  
458 (O'Reilly 2018), possibly modulating ability to predict the NAO (Weishiemer et al. 2019),

459 although sampling variability can also give rise to such long-term changes in teleconnections  
460 (Yun and Timmermann 2018).

461

462 **Modelling issues.**

463 *Subseasonal to Seasonal*

464 Because S2S operational prediction is a relatively new enterprise, considerable efforts focusing  
465 on fundamental aspects of forecast system design are occurring at operational centers  
466 worldwide (Takaya, 2019). One major emphasis consists of methods to represent the  
467 uncertainty in initial conditions (bred vector, singular vector, ensemble data assimilation) and  
468 model physics (stochastic physics, Leutbecher et al. 2018). In addition, configurations of real-  
469 time forecasts and hindcasts, including ensemble size, ensemble strategy (lagged ensemble  
470 with different initial times or burst ensemble with a common initial time) and hindcast period,  
471 impact forecast quality and ability to evaluate the performance of the hindcast. Identifying  
472 suitable compromises and trade-offs in forecast system design is a challenge under practical  
473 constraints for operational activities (costs, priorities, timeliness) and demands further  
474 research.

475

476 From the modelling perspective, multiple operational centers are moving towards a unified, or  
477 “seamless” coupled forecast system that can be applied across timescales from days to seasons  
478 or longer. More S2S models are incorporating ocean and sea-ice components, and becoming  
479 increasingly complex and complete in representing coupled processes in the Earth system. On  
480 the other hand, poor representation of model physics, in particular clouds (Morcrette et al.

481 2018), results in model drifts and biases in surface land and ocean temperatures, which is a  
482 long-standing modeling issue that can degrade the skill of S2S predictions (Vitart and  
483 Balmaseda, 2017). Improvements in cloud parameterizations (Stan and Straus, 2019) and in  
484 representing the diurnal cycle of the atmospheric boundary layers are crucial for advancing S2S  
485 modeling. The Earth system modeling approach poses another challenge to initialize the ocean  
486 and sea ice components with high accuracy; for example there is a relatively large dispersion of  
487 initialized sea ice fields in current S2S models (Chevallier et al. 2017, Zampieri et al. 2018).

488 Another important S2S modeling issue is predicting the MJO, owing to its importance as a  
489 source of subseasonal predictability (H. Kim et al. 2018). Multi-model evaluations have shown  
490 that S2S models have difficulties in representing MJO propagation across the Maritime  
491 Continent. Process-oriented diagnostics (Maloney et al. 2019) have identified a dry bias in the  
492 lower troposphere as one of the causes for the poor MJO propagation through weakening the  
493 horizontal moisture gradient over the Indian Ocean and western Pacific (Lim et al. 2018) and  
494 dampening the organization and propagation of the MJO. A recharge process whereby moisture  
495 builds up in the lower troposphere during the suppressed convection phase of the MJO, and  
496 that is key for MJO propagation around the Maritime Continent in boreal winter, is  
497 underrepresented in S2S models due to the dry bias (Kim 2017). Ocean coupling is another  
498 important process for the MJO (DeMott et al. 2015), and several studies have demonstrated  
499 that ocean coupling can improve MJO propagation and enhance predictive skill in models.

500

501 Poor vertical resolution, low model lid height, inadequate orographic and non-orographic  
502 gravity wave parameterizations, and biases in the tropospheric mean state (e.g., the location of

503 stationary Rossby waves) could limit the predictive skill from stratosphere-troposphere  
504 coupling processes (Tripathi et al. 2015; Butler et al. 2016), but new generations of prediction  
505 systems have rapidly improved in many of these areas. Future model development could  
506 prioritize improved representation of orographic and non-orographic gravity wave drag and an  
507 internally-generated QBO (Butchart et al. 2018). Better understanding of stratosphere-  
508 troposphere coupling processes and the role of the stratosphere on surface skill could be  
509 gained through case studies and stratospheric nudging experiments (Hansen et al. 2017).  
510 Improved observations of the stratosphere (e.g., aerosols and chemistry) and other climate  
511 components may improve S2S predictions. Finally, there is potential for modeling of  
512 stratospheric ozone chemistry which provides surface temperature predictability on S2S time  
513 scales due to its influence on high-latitude stratospheric circulation anomalies together with  
514 their lagged surface impacts (Stone et al. 2019). Although that may currently be too resource-  
515 intensive due to the many species and reactions that must be modeled, emerging machine-  
516 learning techniques may provide pathways for incorporating chemistry-climate information into  
517 S2S forecasts (Nowack et al. 2018).

518

### 519 *Seasonal to decadal*

520 Modeling issues for S2D prediction naturally overlap with those for S2S prediction. However,  
521 the longer time scales of S2D prediction lead to a greater emphasis on representing slower  
522 climate variations such as ENSO and AMV, and greater attention to reducing model biases in  
523 the ocean that may take months to years to develop. Increased model resolution can reduce  
524 model biases as illustrated in Fig. 5 (Jia et al. 2015; Müller et al. 2018), and improve skill

525 (Prodhomme et al. 2016b; Schuster et al. 2019; Infanti and Kirtman 2019), although the greater  
526 computational cost is not always justified (Scaife et al. 2019). More fundamental strategies  
527 involve analyzing/understanding model biases, before attempting to correct them a priori or a  
528 posteriori. Such analysis methods include comparing hindcasts with observations and multi-  
529 decadal historical or other simulations to distill causation for model errors, such as in the  
530 tropical Pacific (Shonk et al. 2018) or Atlantic (Voldoire et al. 2019). Similarly, errors in modeled  
531 variability or teleconnection patterns can be characterized by examining their evolution with  
532 lead time. Model biases can be corrected both through simple methods such as statistical bias  
533 correction and anomaly coupling (Tonizzo and Koseki, 2018), and more complex methods such  
534 as supermodeling, through which multiple models exchange information during a climate  
535 simulation (Shen et al. 2016).

536

537 Performance of S2D predictions is strongly tied to initialization of model components beyond  
538 the lower atmosphere. For example, stratospheric initial conditions are a source of seasonal  
539 winter NAO skill (e.g., O'Reilly et al. 2019; Nie et al. 2019) as illustrated in Fig. 6, and ocean  
540 initial conditions are crucial for skillfully predicting ENSO (Balmaseda and Anderson 2009), as  
541 well as decadal variability in the subpolar North Atlantic (Yeager and Robson, 2017; Borchert et  
542 al. 2018). However, initialization using full-field observational values can lead to initial shocks  
543 affecting skill (Kröger et al. 2018) and in such cases initialization combining observed anomalies  
544 with the model's own climatology can be beneficial until underlying model errors can be  
545 reduced (Volpi et al. 2017). Basic initialization strategies continue to be an active research area  
546 particularly for decadal prediction (Brune et al. 2018), and methods extending to forecast runs

547 such as the ensemble dispersion filter which replaces the ensemble members with the  
548 ensemble mean every three months (Kadlow et al. 2017) are also being explored. Comparisons  
549 that apply different initialization methods to the same model can yield valuable insights  
550 (Polkova et al. 2019); further issues specific to the initialization of the land, ocean, and sea ice  
551 components are considered in the next section.

552  
553 Tackling these diverse and persistent modeling issues effectively will require sustained effort, as  
554 simple model-specific solutions may not cure the underlying problems, and ideally this should  
555 involve coordination between the S2S/S2D prediction, climate modelling, and data assimilation  
556 communities.

557  
558 **Initialization issues.**

559 *Atmosphere initialization*

560 Accurate atmospheric model initialization is a basic requirement for numerical weather  
561 prediction because atmospheric initial conditions are the primary source of predictability on  
562 time scales less than a week or two (Fig. 1). It is enabled by sophisticated data assimilation  
563 systems that are the result of decades of advancement (Bauer et al. 2015). Subseasonal and  
564 seasonal prediction systems generally initialize their atmospheric components by such means,  
565 with the additional requirement that historical observations must be assimilated similarly to  
566 produce reanalyses that are used to initialize hindcasts. Because in situ and remotely sensed  
567 atmospheric observations are relatively dense there is generally good agreement between  
568 different reanalyses for the modern era implying relatively low uncertainty at heights below

569 about 10 hPa, although temporal inconsistencies can result from changes in observing systems  
570 (Long et al. 2017). Because atmospheric initial conditions contribute less to predicability on  
571 multi-annual time scales, some decadal prediction systems do not initialize the atmosphere  
572 (e.g., Yeager et al. 2018).

573

#### 574 *Land initialization*

575 Climatically important land variables such as soil moisture and snow can be initialized by driving  
576 land surface models with observed atmospheric fields (e.g., Koster et al. 2009; Sospedra-  
577 Alfonso et al. 2016a) or, more directly, assimilation of land observations principally from  
578 satellites (Bilodeau et al. 2016; Muñoz-Sabater et al. 2019; Toure et al. 2018). Yet predictability  
579 from land surface states is being harvested only to the extent that land initial conditions and  
580 the relevant processes are represented realistically in forecast models (Koster et al. 2011;  
581 Ardilouze et al. 2017). Historically, land surface and atmospheric models are developed  
582 separately and their coupled behavior is not calibrated or validated (Dirmeyer et al. 2019), so  
583 that coupled processes are often not represented accurately (Dirmeyer et al. 2018b).

584

585 There are also observational limitations. In situ measurements of soil moisture are of varying  
586 quality and uneven distribution, and are not designed for real-time operational use (Dorigo et  
587 al. 2011). Satellite soil moisture monitoring (Entekhabi et al. 2010; Kerr et al. 2010), provides  
588 either very shallow or total column measurements including groundwater (Li et al. 2012), and is  
589 subject to uncertainties caused by vegetation, etc. (Al-Yaari et al. 2017). By contrast, soil  
590 moisture in forecast models is mainly a gross reservoir for the surface water balance, and its



591 variations do not represent all of the observed processes, particularly at sub-grid scales.  
592 Therefore model soil moisture is only a crude representation of reality, although it still contains  
593 useful information that can be largely consistent across different land models (Koster et al.  
594 2009).

595

596 Climate forecasts can be improved by making high-quality land state observations an  
597 operational priority for real-time reporting, and planning for long-term continuity in satellite  
598 monitoring (Balsamo et al. 2018). This includes vegetation, especially as its interannual  
599 variability and cycles of agricultural planting and harvest are not represented and can affect  
600 surface fluxes and predictions (Alessandri et al. 2017). In addition, realistic snow initialization  
601 can positively impact subseasonal predictions of surface temperatures (e.g., F. Li et al. 2019).  
602 Along with coupled land-atmosphere model development (Santanello et al. 2018), such efforts  
603 would facilitate improved predictions on weather to subseasonal time scales, as demonstrated  
604 by numerous forecast model-based sensitivity studies such as that of Koster et al. (2011).

605

#### 606 *Ocean and sea ice initialization*

607 The importance of initializing the oceans stems from their relatively long thermal and dynamical  
608 time scales, through which they play an essential role in S2D climate predictability (Cassou et al.  
609 2017). In addition, the oceans can influence S2S variability, for example through air-sea  
610 interactions affecting the MJO (DeMott et al. 2015) and mesoscale eddy impacts on  
611 atmospheric circulation (Saravanan and Chang 2019). Predicting future ocean evolution,  
612 especially on S2D time scales, requires estimates of 3D ocean states for initialization. This in

613 turn requires a data assimilation method (usually in conjunction with a dynamical model) to  
614 constrain ocean state estimates based on available observations. Similar considerations apply  
615 to state estimates of sea ice. Comparisons of different ocean and sea ice state estimates as in  
616 Fig. 7 can point to variables and regions for which they are most robust, as well as to where  
617 uncertainties are relatively large (Balmaseda et al. 2015; Chevallier et al. 2017). Observing  
618 system experiments in which certain observations are withheld have shown for example that  
619 data from tropical ocean moorings positively impacts state estimates even when Argo float  
620 data is also available (Fujii et al. 2015).

621  
622 Recent enhancements in observing capabilities are enabling improvements in ocean and sea ice  
623 state estimates, potentially leading to more accurate initial conditions and hence better  
624 forecasts. For example, assimilation of satellite measurements of sea surface salinity (SSS) leads  
625 to improvements in tropical Pacific ocean states and ENSO forecasts in experiments using an  
626 intermediate-complexity coupled model (Hackert et al. 2019), whereas assimilation of satellite-  
627 derived sea ice thickness (SIT) measurements has shown potential for improving sea ice  
628 forecasts in operational seasonal forecasting systems (Chen et al. 2017; Blockley and Peterson,  
629 2018). A major limitation is that these data sources have been available for less than a decade,  
630 whereas considerably longer hindcast periods are required for forecast post-processing and skill  
631 assessment, and temporal consistency of observational data used for initialization is required to  
632 avoid artificial biases between hindcasts and forecasts. Forecasts thus continue to be initialized  
633 typically without assimilation of SSS or SIT, from initial conditions that deviate appreciably from

634 available observations especially for SIT (Uotila et al. 2019). This motivates alternative  
635 approaches for initializing SIT over multidecadal hindcast periods (Dirkson et al. 2017).

636

### 637 *Coupled data assimilation*

638 The atmosphere, land, ocean and sea ice components of climate prediction models have often  
639 been initialized individually, without coupling. However, such an approach does not make  
640 optimal use of observations, which may exert influences across the interfaces of the model  
641 components. In addition, physical inconsistencies between the separately initialized  
642 components may lead to rapid adjustments, or shocks. To overcome these limitations attention  
643 has increasingly turned toward developing coupled data assimilation methods that treat  
644 multiple components, such as atmosphere and ocean, simultaneously using observations from  
645 each (Penny and Hamill 2017). Such methods are termed weakly or strongly coupled (Penny et  
646 al. 2017). Weakly coupled methods apply assimilation independently to each model component  
647 within the coupled model, so that the components may exchange information across their  
648 interfaces. Such techniques have shown promise for reducing shocks (Mulholland et al. 2015),  
649 and have begun to be applied operationally (e.g., Browne et al. 2019). Strongly coupled  
650 methods apply assimilation to multiple model components in an integrated manner, so that  
651 observations assimilated in one component can directly influence others. Such methods  
652 remain experimental and thus far have been applied mainly in simplified models (e.g., Penny et  
653 al. 2019).

654

### 655 **Ensemble predictions and forecast information.**

656 *Subseasonal to Seasonal*

657 In contrast to ensemble weather forecasts, a consolidated verification strategy for S2S  
658 predictions is not yet established, and developing such a framework that encompasses  
659 important forecast attributes such as accuracy, association, discrimination, reliability, and  
660 resolution has thus emerged as a priority (Coelho et al. 2018). (Accuracy measures error, or  
661 distance between forecast and observed values; association measures strength of the linear  
662 relationship between forecast and observation as through temporal or spatial correlations;  
663 discrimination measures by how much forecasts differ given different outcomes; reliability  
664 measures how well forecast probabilities correspond to observed frequencies of occurrence;  
665 resolution measures by how much outcomes differ given different forecast probabilities.  
666 Forecast quality encompasses all these attributes, whereas skill indicates quality relative to  
667 some benchmark such as persisted anomalies or climatological probabilities.) As for seasonal  
668 predictions, a purpose of S2S hindcasts is to provide a larger sample for more confident  
669 verification statistics than real time forecasts because they cover more years. However,  
670 because S2S hindcasts are initialized using re-analysis and most often have a smaller ensemble  
671 size, their verification generally underestimates real-time forecast quality. Operational centres  
672 are encouraged to compute and monitor verification statistics based both on hindcasts and  
673 real-time forecasts.

674

675 As has been demonstrated for seasonal prediction, S2S multi-model ensembles (MMEs)  
676 generally outperform individual models (Vigaud et al. 2017; Pegion et al. 2019). Currently, the

677 S2S and SubX MME projects are providing testbeds for research<sup>3</sup> as well as a foundation for  
678 operational use (Vitart and Robertson 2019; Pegion et al. 2019). One focus for exploiting such  
679 datasets is developing calibration procedures, post-processing steps that improve the  
680 properties of probabilistic forecasts, to enable S2S ensemble forecasts to provide reliable  
681 probabilities for particular conditions occurring or thresholds being exceeded, especially for  
682 extreme events. The varied current choices among S2S project modelling systems for hindcast  
683 and near real time initialization dates, hindcast period and ensemble size is, however, limiting  
684 advances in developing multi-model calibration and combination procedures. In addition, the  
685 value of these datasets for research would be enhanced if more comprehensive stratospheric  
686 data were to be available across models.

687  
688 S2S ensemble forecasts have shown promise in providing useful predictions and early warnings  
689 for high impact climate and weather events including severe heat waves and cold spells, as well  
690 as regional probabilities of the occurrence of tropical storms as illustrated in Fig. 8 (Vitart and  
691 Robertson 2018). Examples include severe cold conditions over Europe associated with the  
692 negative phase of the NAO, whose useful predictability into week 3 is enhanced by tropical–  
693 extratropical teleconnections resulting from MJO activity (Ferranti et al. 2018), and atmospheric  
694 rivers, plumes of intense water vapor transport that often trigger weather and hydrologic  
695 extremes and are especially predictable at lead times of 3 to 5 weeks during certain MJO and  
696 QBO phase combinations (Baggett et al. 2017). While modest overall skill at ranges longer than

---

<sup>3</sup> Hindcast and near real-time forecast data are available from S2S at [www.s2sprediction.net](http://www.s2sprediction.net) and from SubX at <http://iridl.ldeo.columbia.edu/SOURCES/.Models/.SubX/>.

697 a week has been found for S2S predictions of springtime Sahelian heat waves including  
698 measures of heat stress, such conditions following a strong El Nino were accurately forecast,  
699 pointing to the tropical Pacific as a source of predictability for extremes in that region (Batté et  
700 al. 2018).

701

702 A global precipitation hindcast quality assessment of the S2S prediction project models (Fig. 9)  
703 was performed by de Andrade et al. (2019). Sub-seasonal prediction quality is modulated by  
704 the MJO, QBO, ENSO in the tropics, changes in large-scale flow in the extra-tropics and  
705 stratospheric tropical and extratropical variability (Butler et al. 2019). It is therefore important  
706 to estimate the predictive skill of such events and identify their impacts on predictions of  
707 weather and weather extremes. Evaluating the conditional prediction quality associated with  
708 the key low frequency variability modes is instrumental for better understanding S2S  
709 predictability mechanisms. For example, MJO predictive skill in the S2S MME ranges between  
710 12 to 36 days and is affected both by the MJO amplitude and phase errors (Vitart 2017; Lim et  
711 al. 2018; H. Kim et al. 2018). Communicating these variations in forecast quality, including if the  
712 forecasts are no better than climatology, is extremely important as users with such knowledge  
713 can better utilize and benefit from the forecast information. Furthermore, capitalizing on  
714 “windows of opportunity” when skill is especially high increases the value of S2S forecasts  
715 (Mariotti et al. 2020), and motivates their frequent initialization (ideally daily).

716

717 *Seasonal to decadal*

718 Limited forecast quality in current S2D ensemble prediction systems motivates research  
719 initiatives that focus on extracting skillful and reliable information from the large amounts of  
720 forecast and hindcast data available to potential users<sup>4</sup>.

721

722 One emerging theme of such research is that S2D prediction systems sometimes underestimate  
723 the predictable signal (Eade et al. 2014; Scaife and Smith 2018). As a result, very large ensembles  
724 that effectively filter out unpredictable noise demonstrate higher skill in predicting phenomena  
725 such as the winter NAO (Scaife et al. 2014b; Dunstone et al. 2016) and seasonal to multi-annual  
726 regional precipitation variations (Dunstone et al. 2018; Yeager et al. 2018) than was previously  
727 thought possible. While very large ensemble sizes hold value for isolating weak predictable  
728 signals, much smaller ensemble sizes are sufficient for skillful prediction of tropical SST, for which  
729 signal to noise ratios are much larger (Zhu et al. 2015). The causes of unrealistically low modeled  
730 predictable signals (sometimes called the “signal to noise paradox”) remain under investigation.  
731 Two hypotheses stemming from hindcast experiments are that winter NAO skill is enhanced by  
732 skillful prediction of a QBO teleconnection that is too weak in models (O’Reilly et al. 2019), and  
733 that transient eddy feedbacks are too weak in models (Scaife et al. 2019). Others based on simple  
734 models suggest that the NAO predictable signal is too weak because climate models switch

---

<sup>4</sup> Seasonal hindcast data from the WCRP Climate-system Historical Forecast Project (CHFP; Tompkins et al. 2017) are available at <http://chfps.cima.fcen.uba.ar/access.php>, and from the North American Multi-Model Ensemble (NMME, Kirtman et al. 2014) including real-time forecasts at <https://iridl.ldeo.columbia.edu/SOURCES/.Models/.NMME/>. Decadal hindcast data from the WCRP Coupled Model Intercomparison Project Phases 5 and 6 are available via <https://esgf-node.llnl.gov/projects/cmip5/> and <https://esgf-node.llnl.gov/projects/cmip6/>.

735 between NAO regimes too rapidly (Strommen and Palmer 2019), or exhibit less persistent NAO  
736 variability than is observed (Zhang and Kirtman 2019).

737  
738 In the case of the winter NAO which is a key source of variability over the mid-latitude North  
739 Atlantic and Europe, another approach to extract relevant information from over-dispersive  
740 ensembles that leads to improved skill is to subsample ensemble members that are close to a  
741 “first guess” statistical prediction of the NAO (Dobrynin et al. 2018); subsampling has shown  
742 potential for improving European summer forecasts as well (Neddermann et al. 2019).

743  
744 Estimating and realizing the predictability of key modes of variability is still a major challenge at  
745 S2D time scales. ENSO is considered one of the most predictable phenomena on multi-seasonal  
746 time scales, but longer-range skill has been viewed as limited. However, multi-year ensemble  
747 predictions have shown evidence of skill in predicting long-lasting La Niña events that follow  
748 warm events up to 24 months ahead (DiNezio et al. 2017; Luo et al. 2017). Challenges in the  
749 initialization of such longer time scale predictions remain, as evidenced by multi-year predictions  
750 in which skill for SST and precipitation over land improves with lead time in some areas,  
751 suggesting that short-term adjustments following initialization may tend to degrade skill (Yeager  
752 et al. 2018).

753  
754 Calibration of ensemble forecasts is a necessary step to reduce the areas for which S2D forecasts  
755 are unreliable and potentially misleading. Combinations of several forecasting systems such as  
756 the North American Multi-Model Ensemble (NMME, Kirtman et al. 2014) are now routinely used



757 to increase ensemble reliability and improve forecast skill. Several recent efforts have explored  
758 weighted multi-model calibration methods to combine ensembles from different models in order  
759 to improve probabilistic seasonal forecasts for temperature and precipitation anomalies as well  
760 as forecast of extremes (Becker 2017). Calibration methods have also been developed for  
761 ensemble decadal hindcasts to adjust both the bias and ensemble spread with a parametric  
762 dependency on lead time and initialization time (Pasternack et al. 2018). Such methods are found  
763 to improve both the conditional bias and probabilistic skill of decadal hindcasts.

764

#### 765 **Climate forecasts for decision making.**

##### 766 *Subseasonal to Seasonal*

767 Many decisions are made on the S2S forecasting timescale, which sits between weather  
768 forecasts and S2D climate outlooks; therefore the continued development of S2S forecasts has  
769 the potential to benefit many sectors of society (Fig. 10). S2S forecasting is a rapidly maturing  
770 discipline, with emerging recognition for both the need and the potential use of forecasts on  
771 this timescale (White et al. 2017). While S2S forecasts are increasingly being used in  
772 government as well as a range of sectors including agriculture, energy, finance, health and  
773 water resource management – more engagement between S2S forecasters and end users is  
774 needed to increase the wider awareness and uptake of S2S forecasts.

775

776 Although scientific knowledge gaps, computational capacity, and gaps in observations and  
777 modeling currently limit the use of S2S forecasts to some degree, by increasingly placing  
778 decision makers at the forefront of S2S forecast development, an improved dialogue between

779 S2S forecasters, developers and end users will accelerate the awareness and application of S2S  
780 forecasts to real-world decision-making.

781

782 To support the increased use of S2S forecasts for decision-making, the following  
783 recommendations were identified for action following the Boulder conference:

- 784 ● A summary of existing stakeholder case studies is planned to be created to demonstrate past  
785 and ongoing ‘success stories’, and support better engagement with end users and  
786 stakeholders. As the S2S forecast needs and associated performance varies greatly between  
787 different sectors and users, the wider community is increasingly working together on the co-  
788 design and production of S2S predictions in order to better meet user needs. Several  
789 applications of S2S forecasts are now being developed in different disciplines, such as the  
790 EU-funded S2S4E project in the energy sector, a quasi-operational excess heat outlook  
791 system in the health sector (Lowe et al. 2016), and S2S hydrologic prediction in the water  
792 management sector. These efforts need to be catalogued and disseminated to guide further  
793 user-driven decision-support products, and to support the continued development of S2S  
794 forecast, verification metrics and related services.
- 795 ● Systematically assessing the relative skill (or lack thereof) of forecasting a series of historical  
796 high-impact events, such as heat waves, extreme rainfall events, or wildfires, on the S2S  
797 timescale would be a useful way to help demonstrate the potential of S2S forecasts to  
798 decision-makers across multiple sectors. At present, such case studies are often ad-hoc and  
799 typically not published in the wider literature; however, a collaborative effort that brings  
800 together a set of demonstrable case studies, involving both forecasters and end users, would

801 fill this gap. For example, a series of ‘tailored narratives’, or ‘storylines’ (approaches that  
802 construct stories of plausible, non-probabilistic climatic futures that relate to a specific  
803 person or sector to counter perceived barriers; e.g., Hazeleger *et al.* 2015), may aid in the  
804 understanding of what S2S forecasts may deliver in the future.

- 805 ● To support the co-design, uptake and use of S2S forecasts, S2Sapp.net is currently being  
806 established as a new network of researchers, modellers and practitioners – an ‘open to all’  
807 global community with a shared aim of exploring and promoting cross-sectoral services and  
808 applications of this new generation of forecasts from across government, academia, and the  
809 private sector.

810

#### 811 *Seasonal to decadal*

812 Research efforts are assessing the value of S2D forecast information for many applications, and  
813 initiatives such as the WMO’s Global Seasonal Climate Update<sup>5</sup> and Annual to Decadal Climate  
814 Update (Kushnir *et al.* 2019) are making such information more widely available. However,  
815 consultation with decision makers is essential in order to tailor forecast information to the needs  
816 and expectations of users.

817

818 Fisheries management is one application for which S2D forecast information holds promise  
819 (Tommasi *et al.* 2017). This is due to reasonable skill for ocean prediction in regions of interest,  
820 coupled with strong influences of S2D climate variability on fish populations. Case studies

---

<sup>5</sup> <https://public.wmo.int/en/our-mandate/climate/global-seasonal-climate-update>

821 employing fisheries management decision frameworks have shown that SST forecast information  
822 can potentially increase fishery yields while reducing the risk of population collapse from  
823 combined effects of environmental factors and overfishing. However, significant challenges  
824 remain for fully realizing this potential. These include a need for improved initialization and  
825 reduced model errors in key ocean regions such as the US Northeast continental shelf, dynamical  
826 downscaling in cases where important spatial scales are not resolved by global models, and  
827 sufficiently accurate observational data for hindcast verification on these scales. In addition,  
828 incorporating biogeochemistry and marine ecosystem components into prediction systems will  
829 expand their potential capabilities, while posing additional verification challenges.

830

831 Another current focus of application-oriented research is water management. Global climate  
832 prediction models have been shown to have skill in predicting the next winter season's snowpack  
833 throughout much of the western US, where spring snowmelt is an essential water resource  
834 (Kapnick et al. 2018; Sospedra-Alfonso et al. 2016b). Because temperature influences snowmelt  
835 and runoff efficiency, skill in seasonal temperature forecasts can provide improved skill for  
836 seasonal water supply forecasts in this region (Lehner et al. 2017). Seasonal forecast skill has also  
837 been demonstrated for monsoon rainfall (e.g., Jain et al. 2019) and drought (Hao et al. 2018) with  
838 potential to inform water management decisions in many regions of the globe. Decadal forecasts  
839 potentially can meet planning horizon needs but currently are less familiar to water managers  
840 than seasonal forecasts and long-term climate projections. Efforts to apply decadal climate  
841 information for water management decisions have included assessing the role of decadal modes  
842 of variability, and using statistically downscaled decadal predictions as hydrological model inputs.

843 Developing information that is credible and compatible with existing decision frameworks is an  
844 important consideration (Towler et al. 2018).

845  
846 Additional sectors for which S2D forecasts are being assessed for decision making include  
847 agriculture (Klemm and McPherson, 2017), energy (demand & wind power generation, Clark et  
848 al. 2017; Lledó et al. 2019), tropical cyclone (Bergman et al. 2019) and coastal flooding (Widlansky  
849 et al. 2017) preparedness, Arctic marine transportation (Stephenson and Pincus 2018), wildfire  
850 risk (Turco et al. 2019), and food security (Funk et al. 2019).

851  
852 Initiatives to develop and deliver climate forecast information range in scale from international,  
853 regional and national (e.g., Marotzke et al. 2016), to individual users, all of which aim to provide  
854 forecast information having practical value for decision makers. In all cases, it is crucially  
855 important that uncertainties are adequately quantified and conveyed in order to avoid any false  
856 sense of certainty and to build trust in forecast information providers, although sometimes this  
857 requires overcoming a preference of users for deterministic information. Additional  
858 considerations are that expectations of users need to be conditioned to generally modest levels  
859 of skill, but that this information can nonetheless be advantageous when applied consistently in  
860 the long term. The likelihood that climate forecast information gets used increases when efforts  
861 are made to build relationships with potential users, and dialogs are opened to enable forecast  
862 products to be co-designed (Kolstad et al. 2019).

863

864 **Cross-cutting issues in S2S and S2D prediction.**

865 *Initialization shock and model error*

866 Model biases are an endemic modeling issue that is common across S2S and S2D prediction  
867 time scales and influence all aspects of the prediction systems – complicating ingestion of  
868 assimilated observations, degrading skill, and necessitating post-processing steps such as bias  
869 correction and calibration for product development and delivery.

870

871 Model biases begin to develop on fast time scales and lead to drifts from the climate  
872 represented by the initial conditions to that of a model’s biased equilibrium state. It has been  
873 extremely hard to understand the mechanisms behind these drifts, and further, pathways for  
874 their diagnosis are not clear although some progress is being made (Sanchez-Gomez et al. 2015;  
875 Shonk et al. 2018; Voltaire et al. 2019). Such difficulties arise due to non-linear interaction  
876 between various physical processes that are parameterized, and because biases could be non-  
877 local in their origin. Long time scales before models’ equilibrium states are attained make  
878 understanding the causes of drifts even harder. The Boulder meeting recognized that the  
879 S2S/S2D prediction community needs to pay particular attention to developing pathways for  
880 understanding the onset of model biases and put together mechanisms (such as summer  
881 schools) to train the next generation of scientists with interest and expertise in climate  
882 modeling and model diagnostics.

883

884 Initialization shocks that arise from imbalances in initial states with respect to the formulation  
885 of the model and can be caused by limitations of observations and data assimilation as well as  
886 model biases were also recognized as a major issue, particularly in the context of decadal

887 predictions. Initialization shocks result in the degradation of initial information that may be the  
888 primary source of predictability for the subsequent forecast. Even after considerable research  
889 and investment in decadal predictions it is still not clear what may be best approaches, such as  
890 between full field vs. anomaly initialization, to retain predictive information in the initial state  
891 while minimizing the influence of initial shocks on the subsequent forecast. The continuing  
892 prominence of model drift and initial shocks as important issues reinforces a long held  
893 sentiment that these are outstanding problems that need to be studied more systematically if  
894 progress in translating inherent predictability into prediction skill is to be made.

895

#### 896 *S2S and S2D research interactions*

897 The examples of interaction among modes of variability across S2S and S2D time scales noted  
898 earlier emphasize the fact that continued interaction and communication across the S2S and  
899 S2D research communities will be important to make progress. Furthering our understanding of  
900 time-scale interactions will require investments in process level understanding of these  
901 phenomena and will not only benefit our understanding about their lower-frequency variations  
902 but will also contribute to improved process level diagnostics of model simulations. Better  
903 understanding of time-scale interactions is likely to require the use of a hierarchy of models,  
904 such as simple linear models to investigate the characteristics of tropical-extratropical  
905 interactions (including their influence on storm tracks), to diagnose possible causes for errors in  
906 their representation in complex GCMs (Dias et al. 2019).

907

908 Another aspect of research interactions across time scales is quantifying the fidelity of models  
909 in S2S and S2D prediction as well as projections of climate on longer time scales based on their  
910 simulation and prediction of shorter time-scale phenomena. The advantage of such an  
911 approach is that much larger samples for predictions of shorter time-scale phenomena are  
912 available, and an assessment of the reliability of such predictions can be used to build  
913 confidence in prediction on longer time-scales. Theoretical basis for extrapolating the reliability  
914 of forecasts across different time scales may also require the use of a hierarchy of models  
915 (Weisheimer and Palmer 2014; Christensen and Berner 2019).

916

#### 917 *Research and operations*

918 Post-processing to improve forecast quality is an important area of research that bears directly  
919 on operational activities. Post-processing is necessary because biases in forecasts can be as  
920 large as the predicted signal, and therefore require the use of bias correction and calibration  
921 techniques to adjust real-time predictions before their delivery to the users. These  
922 requirements are shared across sub-seasonal to decadal prediction time-scales, however  
923 because of different levels of experience (seasonal predictions having the longest history) the  
924 opportunity for cross-community interactions was recognized. Some aspects for post-  
925 processing are specific to time-scale, for example, bias correction for decadal predictions  
926 requires methods to account for the non-stationarity of climate, and research needs to develop  
927 such methods were stressed.

928



929 Necessity for post-processing requires an extensive set of hindcasts to accompany real-time  
930 predictions. Because of limited resources, decisions about hindcast period, ensemble size and  
931 forecast start dates are not straightforward and call for further guidance from the research  
932 community. Such questions about the operational infrastructure for long-range prediction  
933 systems, including ensemble generation techniques and recommendations for harmonizing  
934 hindcast and real time forecast production, provide an opportunity to link operational and  
935 research communities that was highlighted during the conference.

936

937 Product development and communicating forecasts to the user community is also a common  
938 thread across the S2S and S2D communities. Communication of probabilistic forecast  
939 information (including confidence in the forecast based on past verifications) to users for their  
940 decision making has been a challenge, and once again there is much to be gained from lessons  
941 learned from the experiences of different communities. Similar challenges and opportunities  
942 also exist in the context of product development that incorporate user needs based on an  
943 ongoing dialog from the very start of the process. In addition, users often wish to have  
944 information on smaller spatial scales than are represented in global climate models. For such  
945 applications either statistical or dynamical downscaling is possible and can be effective in  
946 reducing local climatological biases, although clear demonstrations that downscaling can  
947 improve the skill of climate predictions remain elusive (e.g., Manzanas et al. 2018).

948

949 In summary, research needs for further development of operational infrastructure, product  
950 generation and communication of probabilistic forecasts were themes often repeated during  
951 the conference.

952

### 953 **Conclusions and the future of subseasonal to decadal prediction**

954 This paper has outlined many commonalities in the prediction of weather and climate across  
955 time scales and Earth system components, and through the value cycle from basic research to  
956 operational delivery.

957

958 The Earth's weather and climate is inherently chaotic and challenges the best currently  
959 available modeling capabilities. There remains however untapped skill, and realizing this skill  
960 will require improvements on numerous fronts. These include fundamental understanding of  
961 fine-scale processes, leading toward their robust parameterization; accurately representing  
962 property exchanges across Earth system components through realistic coupling limiting  
963 systematic errors; sustained Earth observing systems and advanced data assimilation methods  
964 enabling balanced initial conditions that avoid shocks and mitigate model drifts; and innovative  
965 numerical and ensemble generation techniques to address model scalability issues. Additional  
966 important avenues toward improved services include development of probabilistic information  
967 for high impact weather and climate events including unprecedented extremes, and optimal  
968 post-processing and data fusion to add value to multi-model ensembles, among many others.

969

970 These challenges are broad but so are opportunities for steady progress, ranging from curiosity-  
971 driven science to the systematic model evaluation and improvement in a collaborative and  
972 open research/operational environment.

973

974 The joint WWRP-WCRP conferences in Boulder clearly demonstrated the benefit in bringing  
975 relevant stakeholders together to cross-fertilize their experience, knowledge, respective issues  
976 and working cultures, which will surely help frame a new and vibrant research portfolio, and  
977 inspire the next generation of science leaders to ensure that society has access to the best  
978 possible weather and climate prediction science.

979

#### 980 **ACKNOWLEDGEMENTS**

981 The International Conferences on Subseasonal to Decadal Prediction on which this paper is  
982 based were sponsored by: US CLIVAR, NSF, UCAR, NCAR and its Climate and Global Dynamics  
983 Laboratory (CGD), NOAA's Climate Variability and Predictability (CVP) and Modeling, Analysis,  
984 Predictions and Projections (MAPP) Programs, Copernicus Climate Change Service, IPSL, and  
985 WWRP/WCRP's Subseasonal-to-Seasonal (S2S) Prediction Project.

986

987

988

989

990

991

992 **REFERENCES**

- 993 Alessandri, A., F. Catalano, M. De Felice, B. Van Den Hurk, F. Doblas Reyes, S. Boussetta, G.  
994 Balsamo, and P. A. Miller, 2017: Multi-scale enhancement of climate prediction over  
995 land by increasing the model sensitivity to vegetation variability in EC-Earth. *Climate*  
996 *Dyn.*, **49**, 1215–1237, <https://doi.org/10.1007/s00382-016-3372-4>.
- 997 Al-Yaari, A., and Coauthors, 2017: Evaluating soil moisture retrievals from ESA’s SMOS and  
998 NASA’s SMAP brightness temperature datasets. *Remote Sens. Environ.*, **193**, 257-273,  
999 <https://doi.org/10.1016/j.rse.2017.03.010>.
- 1000 Ardilouze, C., and Coauthors, 2017: Multi-model assessment of the impact of soil moisture  
1001 initialization on mid-latitude summer predictability. *Climate Dyn.*, **49**, 3959-3974,  
1002 <https://doi.org/10.1007/s00382-017-3555-7>.
- 1003 Ardilouze, C., L. Batté, M. Déqué, E. van Meijgaard, and B. van den Hurk, 2019: Investigating the  
1004 impact of soil moisture on European summer climate in ensemble numerical  
1005 experiments. *Climate Dyn.*, **52**, 4011-4026, <https://doi.org/10.1007/s00382-018-4358-1>.
- 1006 Ayarzaguen, B., and Coauthors, 2018: No robust evidence of future changes in major  
1007 stratospheric sudden warmings: a multi-model assessment from CCM1. *Atmos. Chem.*  
1008 *Phys.*, **18**, 11277–11287. <http://doi.org/10.5194/acp-18-11277-2018>.
- 1009 Baggett, C., E. A. Barnes, E. Maloney, and B. Mundhenk, 2017: Advancing Atmospheric River  
1010 Forecasts into Subseasonal Timescales. *Geophys. Res. Lett.*, **44**, 7528–7536,  
1011 <https://doi.org/10.1002/2017GL074434>.
- 1012 Baggett, C.F., K. M. Nardi, S. J. Childs, S. N. Zito, E. A. Barnes, and E. D. Maloney, 2018: Skillful  
1013 subseasonal forecasts of weekly tornado and hail activity using the Madden-Julian

1014 Oscillation. *J. Geophys. Res. Atmos.*, **123**, 661–675,  
1015 <https://doi.org/10.1029/2018JD029059>.

1016 Balmaseda, M. A., and D. Anderson, 2009: Impact of initialization strategies and observations  
1017 on seasonal forecast skill. *Geophys. Res. Lett.*, **36**, L01701,  
1018 <https://doi.org/10.1029/2008GL035561>.

1019 Balmaseda, M. A., and Coauthors, 2015: The Ocean Reanalyses Intercomparison Project (ORA-  
1020 IP). *J. Oper. Oceanogr.*, **8** (Suppl.), s80–s97,  
1021 <https://doi.org/10.1080/1755876X.2015.1022329>.

1022 Balsamo, G., and Coauthors, 2018: Satellite and in situ observations for advancing global Earth  
1023 surface modelling: A Review. *Remote Sensing*, **10**, 2038,  
1024 <https://doi.org/10.3390/rs10122038>.

1025 Barnston, A. G., M. K. Tippett, M. Ranganathan, and M. L’Heureux, 2017: Deterministic skill of  
1026 ENSO predictions from the North American Multimodel Ensemble. *Climate Dyn.*,  
1027 <https://doi.org/10.1007/s00382-017-3603-3>.

1028 Batté L., C. Ardilouze, and M. Déqué, 2018: Forecasting West African heat waves at sub-  
1029 seasonal and seasonal time scales. *Mon. Wea. Rev.*, **146**, 889–907,  
1030 <https://doi.org/10.1175/MWR-D-17-0211.1>.

1031 Bauer, P., A. Thorpe, and G. Brunet, 2015: The quiet revolution of numerical weather  
1032 prediction. *Nature*, **525**, 47–55, <https://doi.org/10.1038/nature14956>.

1033 Becker, E. J., 2017: Prediction of short-term climate extremes with a multimodel ensemble.  
1034 *Climate Extremes: Patterns and Mechanisms*, S.-Y. Wang et al. Eds., John Wiley & Sons,  
1035 Inc., 347–359, <https://doi.org/10.1002/9781119068020.ch21>.

1036 Bellucci, A., and Coauthors, 2015: Advancements in decadal climate predictability: The role of  
1037 nonoceanic drivers. *Rev. Geophys.*, **53**, 165–202,  
1038 <https://doi.org/10.1002/2014RG000473>.

1039 Bergman, D. L., L. Magnusson, J. Nilsson, and F. Vitart, 2019: Seasonal Forecasting of Tropical  
1040 Cyclone Landfall Using ECMWF’s System 4. *Wea. Forecasting*, **34**, 1239–1255,  
1041 <https://doi.org/10.1175/WAF-D-18-0032.1>.

1042 Beverley, J. D., S. J. Woolnough, L. H. Baker, S. J. Johnson, and A. Weisheimer, 2019: The  
1043 northern hemisphere circumglobal teleconnection in a seasonal forecast model and its  
1044 relationship to European summer forecast skill. *Climate Dyn.*, **52**, 3759–3771,  
1045 <https://doi.org/10.1007/s00382-018-4371-4>.

1046 Bilodeau, B., M. Carrera, A. Russell, X. Wang, and S. Belair, 2016: Impacts of SMAP data in  
1047 Environment Canada’s Regional Deterministic Prediction System. *2016 IEEE*  
1048 *International Geoscience and Remote Sensing Symposium (IGARSS)*, 5233–5236,  
1049 <https://doi.org/10.1109/IGARSS.2016.7730363>.

1050 Blockley, E. W., and K. A. Peterson, 2018: Improving Met Office seasonal forecasts of Arctic sea  
1051 ice using assimilation of CryoSat-2 thickness. *Cryosphere*, **12**, 3419–3438,  
1052 <https://doi.org/10.5194/tc-12-3419-2018>.

1053 Boer, G. J., and Coauthors, 2016: The Decadal Climate Prediction Project (DCPP) contribution to  
1054 CMIP6. *Geosci. Model Dev.*, **9**, 3751–3777, <https://doi.org/10.5194/gmd-9-3751-2016>.

1055 Booth, B. B. B., N. J. Dunstone, P. R. Halloran, T. Andrews, and N. Bellouin, 2012: Aerosols  
1056 implicated as a prime driver of twentieth-century North Atlantic climate variability.  
1057 *Nature*, **484**, 228–232, <https://doi.org/10.1038/nature10946>.

1058 Borchert, L., W. A. Müller, and J. Baehr, 2018: Atlantic Ocean Heat Transport Influences  
1059 Interannual-to-Decadal Surface Temperature Predictability in the North Atlantic Region.  
1060 *J. Clim.*, **31**, 6763–6782, <https://doi.org/10.1175/JCLI-D-17-0734.1>.

1061 Browne, P. A., P. de Rosnay, H. Zuo, A. Bennett, AND A. Dawson, 2019: Weakly Coupled Ocean–  
1062 Atmosphere Data Assimilation in the ECMWF NWP System. *Remote Sens.*, **11**, 234,  
1063 <https://doi.org/10.3390/rs11030234>.

1064 Brune, S., A. Düsterhus, H. Pohlmann, W. A. Müller, and J. Baehr, 2017: Time dependency of the  
1065 prediction skill for the North Atlantic subpolar gyre in initialized decadal hindcasts.  
1066 *Climate Dyn.*, **51**, 1947–1970, <https://doi.org/10.1007/s00382-017-3991-4>.

1067 Buckley, M. W., T. DelSole, M. S. Lozier, and L. Li, 2019: Predictability of North Atlantic sea  
1068 surface temperature and upper-ocean heat content, *J. Climate*, **32**, 3005–3023,  
1069 <https://doi.org/10.1175/JCLI-D-18-0509.1>.

1070 Butchart, N., and Coauthors, 2018: Overview of experiment design and comparison of models  
1071 participating in phase 1 of the SPARC Quasi-Biennial Oscillation initiative (QBOi). *Geosci.*  
1072 *Model Dev.*, **11**, 1009–1032, <https://doi.org/10.5194/gmd-11-1009-2018>.

1073 Butler, A. H., and Coauthors, 2016: The Climate-System Historical Forecast Project: Do  
1074 stratosphere-resolving models make better seasonal climate predictions in boreal  
1075 winter? *Quart. J. Roy. Meteor. Soc.*, **142**, 1413–1427, <https://doi.org/10.1002/qj.2743>.

1076 Butler, A., and Coauthors, 2019: Sub-seasonal Predictability and the Stratosphere. *Sub-Seasonal*  
1077 *to Seasonal Prediction*, A. W. Robertson & F. Vitart, Eds.. Elsevier, 223–241,  
1078 <https://doi.org/10.1016/B978-0-12-811714-9.00011-5>.

1079 Cai, W., and Coauthors, 2019: Pantropical climate interactions. *Science*, **363**, eaav4236,  
1080 <https://doi.org/10.1126/science.aav4236>.

1081 Capotondi, A., and Coauthors, 2015: Understanding ENSO diversity. *Bull. Amer. Meteor. Soc.*,  
1082 **96**, 921–938, <https://doi.org/10.1175/BAMS-D-13-00117.1>.

1083 Caron, L.-P., L. Hermonson, A. Dobbin, J. Imbers, L. Lledó L, and G. A. Vecchi, 2017: How skilful  
1084 are the multi-annual forecasts of Atlantic hurricane activity? *Bull. Amer. Meteor. Soc.*,  
1085 **99**, 403–413, <https://doi.org/10.1175/bams-d-17-0025.1>.

1086 Cassou, C., Y. Kushnir, E. Hawkins, A. Pirani, F. Kucharski, I. Kang, and N. Caltabiano, 2017:  
1087 Decadal climate variability and predictability: Challenges and opportunities. *Bull. Amer.*  
1088 *Meteor. Soc.*, **99**, 479–490, <https://doi.org/10.1175/BAMS-D-16-0286.1>.

1089 Chen, X., J. Ling, and C. Li, 2016: Evolution of the Madden–Julian oscillation in two types of El  
1090 Niño. *J. Climate*, **29**, 1919–1934, <https://doi.org/10.1175/JCLI-D-15-0486.1>.

1091 Chen, Z., J. Liu, M. Song, Q. Yang, and S. Xu, 2017: Impacts of assimilating satellite sea ice  
1092 concentration and thickness on Arctic sea ice prediction in the NCEP Climate Forecast  
1093 System. *J. Climate*, **30**, 8429–8446, <https://doi.org/10.1175/JCLI-D-17-0093.1>.

1094 Chevallier, M., and Coauthors, 2017: Intercomparison of the Arctic sea ice cover in global  
1095 ocean–sea ice reanalyses from the ORA-IP project. *Climate Dyn.*, **49**, 1107–1136,  
1096 <https://doi.org/10.1007/s00382-016-2985-y>.

1097 Chevallier, M., F. Massonnet, H. Goessling, V. Guémas, and T. Jung, 2019: The Role of Sea Ice in  
1098 Sub-seasonal Predictability. *Sub-Seasonal to Seasonal Prediction*, A. W. Robertson & F.  
1099 Vitart, Eds., Elsevier, 201-221, <https://doi.org/10.1016/B978-0-12-811714-9.00010-3>.



1100 Chikamoto, Y., A. Timmermann, M. J. Widlansky, M. A. Balmaseda, and L. Stott, 2017: Multi-  
1101 year predictability of climate, drought, and wildfire in southwestern North America. *Sci.*  
1102 *Rep.*, **7**, 6568, <https://doi.org/10.1038/s41598-017-06869-7>.

1103 Christensen, H. M., and J. Berner, 2019: From reliable weather forecasts to skilful climate  
1104 response: A dynamical systems approach. *Quart. J. Roy. Meteor. Soc.*, **145**, 1052-1069,  
1105 <https://doi.org/10.1002/qj.3476>.

1106 Clark, R. T., P. E. Bett, H. E. Thornton, and A. A. Scaife, 2017: Skilful seasonal predictions for the  
1107 European energy industry. *Environ. Res. Lett.*, **12**, 12 024002,  
1108 <https://doi.org/10.1088/1748-9326/aa57ab>.

1109 Coelho, C. A. S., M. A. F. Firpo, and F. M. de Andrade, 2018: A verification framework for South  
1110 American sub-seasonal precipitation predictions, *Meteorologische Zeitschrift*, **27**, 503 -  
1111 520, <https://doi.org/10.1127/metz/2018/0898>.

1112 de Andrade, F. M., C. A. S. Coelho, and I. F. A. Cavalcanti, 2019: Global precipitation hindcast  
1113 quality assessment of the Subseasonal to Seasonal (S2S) prediction project models.  
1114 *Climate Dyn.*, **52**, 5451–5475, <https://doi.org/10.1007/s00382-018-4457-z>.

1115 DeFlorio, M., D. Waliser, B. Guan, F. Ralph, and F. Vitart, 2019: Global evaluation of atmospheric  
1116 river subseasonal prediction skill. *Climate Dyn.*, **52**, 3039-3060,  
1117 <https://doi.org/10.1007/s00382-018-4309-x>

1118 DelSole, T., and M. Tippett, 2016: Forecast comparison based on random walks. *Mon. Wea.*  
1119 *Rev.*, **144**, 615–626, <https://doi.org/10.1175/MWR-D-15-0218.1>.

1120 DelSole, T., L. Trenary, M. K. Tippett, and K. Pegion, 2017: Predictability of week-3–4 average  
1121 temperature and precipitation over the contiguous United States. *J. Climate*, **30**, 3499–  
1122 3512, <https://doi.org/10.1175/JCLI-D-16-0567.1>.

1123 DeMott, C. A., N. P. Klingaman, and S. J. Woolnough, 2015: Atmosphere-ocean coupled  
1124 processes in the Madden-Julian oscillation. *Rev. Geophys.*, **53**, 1099–1154,  
1125 <https://doi.org/10.1002/2014RG000478>.

1126 Dias, D. F., A. Subramanian, L. Zanna, and A. J. Miller, 2019: Remote and local influences in  
1127 forecasting Pacific SST: A linear inverse model and a multimodel ensemble study.  
1128 *Climate Dyn.*, **52**, 3183–3201, <https://doi.org/10.1007/s00382-018-4323-z>.

1129 DiNezio and Coauthors, 2017: A 2 year forecast for a 60–80% chance of La Niña in 2017–2018.  
1130 *Geophys. Res. Lett.*, **44**, 11,624–11,635, <https://doi.org/10.1002/2017GL074904>.

1131 DiNezio, P. N., C. Deser, Y. Okumura, and A. Karspeck, 2017: Predictability of 2-year La Niña  
1132 events in a coupled general circulation model. *Climate Dyn.*, **49**, 4237–4261,  
1133 <https://doi.org/10.1007/s00382-017-3575-3>.

1134 Dirkson, A., W. J. Merryfield, and A. Monahan, 2017: Impacts of sea ice thickness initialization  
1135 on seasonal Arctic sea ice predictions. *J. Climate*, **30**, 1001–1017,  
1136 <https://doi.org/10.1175/JCLI-D-16-0437.1>.

1137 Dirmeyer, P. A., and S. Halder, 2016: Sensitivity of numerical weather forecasts to initial soil  
1138 moisture variations in CFSv2. *Wea. Forecasting*, **31**, 1973–1983,  
1139 <https://doi.org/10.1175/WAF-D-16-0049.1>.

1140 Dirmeyer, P. A., and S. Halder, 2017: Application of the land–atmosphere coupling paradigm to  
1141 the operational Coupled Forecast System (CFSv2). *J. Hydrometeor.*, **18**, 85–108,  
1142 <https://doi.org/10.1175/JHM-D-16-0064.1>.

1143 Dirmeyer, P. A., S. Halder, and R. Bombardi, 2018a: On the Harvest of Predictability from Land  
1144 States in a Global Forecast Model. *J. Geophys. Res.*, **123**, 13,111–13,127,  
1145 <https://doi.org/10.1029/2018JD029103>.

1146 Dirmeyer, P. A., and Coauthors, 2018b: Verification of land–atmosphere coupling in forecast  
1147 models, reanalyses, and land surface models using flux site observations. *J.*  
1148 *Hydrometeor.*, **19**, 375–392, <https://doi.org/10.1175/JHM-D-17-0152.1>.

1149 Dirmeyer, P. A., P. Gentine, M. B. Ek, and G. Balsamo, 2019: Land Surface Processes Relevant to  
1150 S2S Prediction. *Sub-Seasonal to Seasonal Prediction*, A. W. Robertson & F. Vitart, Eds.,  
1151 Elsevier, 166–182, <https://doi.org/10.1016/B978-0-12-811714-9.00008-5>.

1152 Dobrynin, M. and Coauthors, 2018: Improved teleconnection-based dynamical seasonal  
1153 predictions of boreal winter. *Geophys. Res. Lett.*, **45**, 3605– 3614,  
1154 <https://doi.org/10.1002/2018GL077209>.

1155 Domeisen, D. I. V., C. I. Garfinkel, and A. H. Butler, 2019a: The teleconnection of El Niño  
1156 Southern Oscillation to the stratosphere. *Rev. Geophys.*,  
1157 <https://doi.org/10.1029/2018RG000596>.

1158 Domeisen, D. I. V., and Coauthors, 2019b: The role of stratosphere-troposphere coupling in sub-  
1159 seasonal to seasonal prediction. Part I: Predictability arising from stratosphere-  
1160 troposphere coupling. *J. Geophys. Res.*, <https://doi.org/10.1029/2019JD030920>.

1161 Domeisen, D. I. V., and Coauthors, 2019c: The role of stratosphere-troposphere coupling in sub-  
1162 seasonal to seasonal prediction. Part II: Predictability arising from stratosphere-  
1163 troposphere coupling. *J. Geophys. Res.*, <https://doi.org/10.1029/2019JD030923>.

1164 Dorigo, W. A., and Coauthors, 2011: The International Soil Moisture Network: a data hosting  
1165 facility for global in situ soil moisture measurements. *Hydrol. Earth Syst. Sci.*, **15**, 1675–  
1166 1698, <https://doi.org/10.5194/hess-15-1675-2011>.

1167 Dunstone, N. J., D. M. Smith, A. Scaife, L. Hermanson, R. Eade, N. Robinson, M. Andrews, and J.  
1168 Knight, 2016: Skilful predictions of the winter North Atlantic Oscillation one year ahead.  
1169 *Nat. Geosci.*, **9**, 809–814, <https://doi.org/10.1038/ngeo2824>.

1170 Dunstone, N. J., and Coauthors, 2018: Skilful seasonal predictions of summer European rainfall.  
1171 *Geophys. Res. Lett.*, **45**, 3246–3254, <https://doi.org/10.1002/2017GL076337>.

1172 Düsterhus, A., 2019: Seasonal statistical-dynamical prediction of the North Atlantic Oscillation  
1173 by probabilistic post-processing. *Nonlin. Processes Geophys. Discuss.*,  
1174 <https://doi.org/10.5194/npg-2019-50>.

1175 Eade, R., D. Smith, A. Scaife, E. Wallace, N. Dunstone, L. Hermanson, and N. Robinson, 2014: Do  
1176 seasonal-to-decadal climate predictions underestimate the predictability of the real  
1177 world? *Geophys. Res. Lett.*, **41**, 5620–5628, <https://doi.org/10.1002/2014GL061146>.

1178 Entekhabi, D., and Coauthors, 2010: The Soil Moisture Active and Passive (SMAP) Mission. *Proc.*  
1179 *IEEE*, **98**, 704–716, <https://doi.org/10.1109/JPROC.2010.2043918>.

1180 Funk, C. and Coauthors, 2019: Recognizing the Famine Early Warning Systems Network: Over 30  
1181 years of drought early warning science advances and partnerships promoting global

1182 food security. *Bull. Amer. Meteor. Soc.*, **100**, 1011–1027, <https://doi.org/10.1175/BAMS->  
1183 [D-17-0233.1](https://doi.org/10.1175/BAMS-D-17-0233.1).

1184 Ferranti, L., L. Magnusson, F. Vitart, and D. S. Richardson, 2018: How far in advance can we  
1185 predict changes in large-scale flow leading to severe cold conditions over Europe?  
1186 *Quart. J. Roy. Meteor. Soc.*, **144**, 1788–1802, <https://doi.org/10.1002/qj.3341>.

1187 Flato, G. M., 2011: Earth System Models: An overview. *Wiley Interdiscip. Rev.: Climate Change*, **2**,  
1188 783–800, <https://doi.org/10.1002/wcc.148>.

1189 Fujii, Y., and Coauthors, 2015: Evaluation of the Tropical Pacific Observing System from the  
1190 ocean data assimilation perspective. *Quart. J. Roy. Meteor. Soc.*, **141**, 2481–2496,  
1191 <https://doi.org/10.1002/qj.2579>.

1192 Garfinkel, C. I., D. W. Waugh, and E. Gerber, 2013: Effect of tropospheric jet latitude on  
1193 coupling between the stratospheric polar vortex and the troposphere. *J. Climate*, **26**,  
1194 2077–2095, <https://doi.org/10.1175/JCLI-D-12-00301.1>.

1195 Garfinkel, C. I., and C. Schwartz, 2017: MJO-related tropical convection anomalies lead to more  
1196 accurate stratospheric vortex variability in subseasonal forecast models. *Geophys. Res.*  
1197 *Lett.*, **44**, 10 054–10 062, <https://doi.org/10.1002/2017GL074470>.

1198 Garfinkel, C. I., C. Schwartz, D. I. V. Domeisen, S.-W. Son, A. H. Butler, and I. P. White, 2018:  
1199 Extratropical Atmospheric Predictability From the Quasi-Biennial Oscillation in  
1200 Subseasonal Forecast Models. *J. Geophys. Res.*, **123**, 7855–7866,  
1201 <https://doi.org/10.1029/2018JD028724>.

1202 Gleixner, S., N. S. Keenlyside, T. D. Demissie, F. Counillon, Y. Wang, and E. Viste, 2017: Seasonal  
1203 predictability of Kiremt rainfall in coupled general circulation models. *Environ. Res. Lett.*,  
1204 **12**, 114016, <https://doi.org/10.1088/1748-9326/aa8cfa>.

1205 Graham, R. J., and Coauthors, 2011: Long-range forecasting and the Global Framework for  
1206 Climate Services. *Climate Res.*, **47**, 47–55, <https://doi.org/10.3354/cr00963>.

1207 Hackert, E., R. M. Kovach, A. J. Busalacchi, and J. Ballabrera-Poy, 2019: Impact of Aquarius and  
1208 SMAP satellite sea surface salinity observations on coupled El Niño/Southern Oscillation  
1209 forecasts. *J. Geophys. Res.*, <https://doi.org/10.1029/2019JC015130>.

1210 Hansen, F., R. J. Greatbatch, G. Gollan, T. Jung, and A. Weisheimer, 2017: Remote control of  
1211 North Atlantic Oscillation predictability via the stratosphere. *Quart. J. Roy. Meteor. Soc.*,  
1212 **143**, 706–719, <https://doi.org/10.1002/qj.2958>.

1213 Hao, Z., V.P. Singh, and Y. Xia, 2018: Seasonal drought prediction: advances, challenges, and  
1214 future prospects. *Rev. Geophys.*, **56**, 108-141, <https://doi.org/10.1002/2016RG000549>.

1215 Hazeleger, W., B. J. J. M. van den Hurk, E. Min, G. J. van Oldenborgh, A. C. Petersen, D. A.  
1216 Stainforth, E. Vasileiadou, L. A. and Smith, 2015: Tales of future weather. *Nat. Climate*  
1217 *Change*, **5**, 107-113, <https://doi.org/10.1038/nclimate2450>.

1218 Henderson, S. A., E. D. Maloney, and S.-W. Son, 2017: Madden–Julian oscillation  
1219 teleconnections: The impact of the basic state and MJO representation in general  
1220 circulation models. *J. Climate*, **30**, 4567–4587, [https://doi.org/10.1175/JCLI-D-16-](https://doi.org/10.1175/JCLI-D-16-0789.1)  
1221 [0789.1](https://doi.org/10.1175/JCLI-D-16-0789.1).

1222 Infanti J. M., and B. P. Kirtman, 2019: A comparison of CCSM4 high-resolution and low-  
1223 resolution predictions for south Florida and southeast United States drought. *Climate*  
1224 *Dyn.*, **52**, 6877–6892, <https://doi.org/10.1007/s00382-018-4553-0>.

1225 Ilyina, T., and P. Friedlingstein, 2016: Biogeochemical Cycles and Climate Change. White Paper on  
1226 the World Climate Research Programme Grand Challenge on Carbon Feedbacks in the  
1227 Climate System, 10 pp, [https://www.wcrp-](https://www.wcrp-climate.org/JSC37/Documents/BGCGC_whitepaper_submission.pdf)  
1228 [climate.org/JSC37/Documents/BGCGC\\_whitepaper\\_submission.pdf](https://www.wcrp-climate.org/JSC37/Documents/BGCGC_whitepaper_submission.pdf)

1229 Jain, S., A. A. Scaife, and A. K. Mitra, 2019: Skill of Indian summer monsoon rainfall prediction in  
1230 multiple seasonal prediction systems. *Climate Dyn.*, **52**, 5291–5301,  
1231 <https://doi.org/10.1007/s00382-018-4449-z>.

1232 Jeong, J.-H., H. W. Linderholm, S.-H. Woo, C. Folland, B.-M. Kim, S.-J. Kim, and D. Chen, 2012:  
1233 Impacts of Snow Initialization on Subseasonal Forecasts of Surface Air Temperature for  
1234 the Cold Season. *J. Climate*, **26**, 1956–1972, <https://doi.org/10.1175/JCLI-D-12-00159.1>.

1235 Jia, L., and Coauthors, 2015: Improved seasonal prediction of temperature and precipitation  
1236 over land in a high-resolution GFDL climate model. *J. Climate*, **28**, 2044–2062,  
1237 <https://doi.org/10.1175/JCLI-D-14-00112.1>.

1238 Kadow, C., S. Illing, I. Kröner, U. Ulbrich, and U. Cubasch, 2017: Decadal climate predictions  
1239 improved by ocean ensemble dispersion filtering. *J. Adv. Model. Earth Syst.*, **9**, 1138–  
1240 1149, <https://doi.org/10.1002/2016MS000787>.

1241 Kang, S. M., Y. Shin, and S.-P. Xie, 2018: Extratropical forcing and tropical rainfall distribution:  
1242 Energetics framework and ocean Ekman advection. *npj Climate Atmos. Sci.*, **1**, 20172,  
1243 <https://doi.org/10.1038/s41612-017-0004-6>

1244 Kapnick, S. B., and Coauthors, 2018: Potential for western US seasonal snowpack prediction.  
1245 *Proc. Natl. Acad. Sci. USA*, **115**, 1180–1185, <https://doi.org/10.1073/pnas.1716760115>.

1246 Karpechko, A.Y., 2018: Predictability of sudden stratospheric warmings in the ECMWF  
1247 extended-range forecast system. *Mon. Wea. Rev.*, **146**, 1063–1075.  
1248 <https://doi.org/10.1175/MWR-D-17-0317.1>.

1249 Kerr, Y. H., and Coauthors, 2010: The SMOS mission: New tool for monitoring key elements of  
1250 the global water cycle. *Proc. IEEE*, **98**, 666–687,  
1251 <https://doi.org/10.1109/JPROC.2010.2043032>.

1252 Khodri, M., and Coauthors, 2017: Tropical explosive volcanic eruptions can trigger El Niño by  
1253 cooling tropical Africa. *Nat. Commun.*, **8**, 778, [https://doi.org/10.1038/s41467-017-](https://doi.org/10.1038/s41467-017-00755-6)  
1254 [00755-6](https://doi.org/10.1038/s41467-017-00755-6).

1255 Kidston, J., A. A. Scaife, S. C. Hardiman, D. M. Mitchell, N. Butchart, M. P. Baldwin, and L. J. Gray,  
1256 2015: Stratospheric influence on tropospheric jet streams, storm tracks and surface  
1257 weather. *Nat. Geosci.*, **8**, 433–440, <https://doi.org/10.1038/ngeo2424>.

1258 Kim, H.-M., 2017: The impact of the mean moisture bias on the key physics of MJO propagation  
1259 in the ECMWF reforecast, *J. Geophys. Res.*, **122**, 7772–7784,  
1260 <https://doi.org/10.1002/2017JD027005>.

1261 Kim, Y.-H., and H.-Y. Chun, 2015: Momentum forcing of the quasi-biennial oscillation by  
1262 equatorial waves in recent reanalyses. *Atmos. Phys. Chem.*, **15**, 6577–6587,  
1263 <https://doi.org/10.5194/acp-15-6577-2015>.

1264 Kim, H., F. Vitart, and D. E. Waliser, 2018: Prediction of the Madden–Julian Oscillation: A  
1265 Review. *J. Climate*, **31**, 9425–9443, <https://doi.org/10.1175/JCLI-D-18-0210.1>.



1266 Kim, W. M., S. G. Yeager, and G. Danabasoglu, 2018: Key role of internal ocean dynamics in  
1267 Atlantic multidecadal variability during the last half century. *Geophys. Res. Lett.*, **45**,  
1268 13,449-13,457, <https://doi.org/10.1029/2018GL080474>.

1269 Kirtman, B., D. Anderson, G. Brunet, I. S. Kang, A. A. Scaife, and D. M. Smith, 2013: Predictions  
1270 from weeks to decades. *Climate Science for Serving Society*, G. R. Asrar and J. W. Hurrell,  
1271 Eds., Springer, 205–235, [https://doi.org/10.1007/978-94-007-6692-1\\_8](https://doi.org/10.1007/978-94-007-6692-1_8).

1272 Kirtman, B. P., and Coauthors, 2014: The North American Multimodel Ensemble: Phase-1  
1273 seasonal-to-interannual prediction; Phase-2 toward developing intraseasonal prediction.  
1274 *Bull. Amer. Meteor. Soc.*, **95**, 585–601, <https://doi.org/10.1175/BAMS-D-12-00050.1>.

1275 Klemm, T., and R. A. McPherson, 2017: The development of seasonal climate forecasting for  
1276 agricultural producers. *Agric. For. Meteor.*, **232**, 384–399,  
1277 <https://doi.org/10.1016/j.agrformet.2016.09.005>.

1278 Kolstad, E. W., and Coauthors, 2019: Trials, errors and improvements in co-production of  
1279 climate services. *Bull. Amer. Meteor. Soc.*, **100**, 1419–1428, [https://doi.org/10.1175/BAMS-D-](https://doi.org/10.1175/BAMS-D-18-0201.1)  
1280 [18-0201.1](https://doi.org/10.1175/BAMS-D-18-0201.1).

1281 Koster, R., and Coauthors, 2004: Regions of strong coupling between soil moisture and  
1282 precipitation. *Science*, **305**, 1138–1140, <https://doi.org/10.1126/science.1100217>.

1283 Koster, R. D., Z. Guo, P. A. Dirmeyer, R. Yang, K. Mitchell, and M. J. Puma, 2009: On the nature  
1284 of soil moisture in land surface models. *J. Climate*, **22**, 4322–4335,  
1285 <https://doi.org/10.1175/2009JCLI2832.1>.

1286 Koster, R. D., and Coauthors, 2011: The second phase of the Global Land–Atmosphere Coupling  
1287 Experiment: Soil moisture contributions to subseasonal forecast skill. *J. Hydrometeor.*,  
1288 **12**, 805–822, <https://doi.org/10.1175/2011JHM1365.1>.

1289 Koster, R. D., Y. Chang, H. Wang, and S. D. Schubert, 2016: Impacts of local soil moisture  
1290 anomalies on the atmospheric circulation and on remote surface meteorological fields  
1291 during boreal summer: A comprehensive analysis over North America. *J. Climate*, **29**,  
1292 7345–7364, <https://doi.org/10.1175/JCLI-D-16-0192.1>.

1293 Kröger, J., and Coauthors, 2018: Full-field initialized decadal predictions with the MPI Earth  
1294 System Model: An initial shock in the North Atlantic. *Clim. Dyn.*, **51**, 2593–2608,  
1295 <https://doi.org/10.1007/s00382-017-4030-1>.

1296 Kushnir, Y., and Coauthors, 2019: Towards operational predictions of the near-term climate.  
1297 *Nat. Climate Change*, **9**, 94–101, <https://doi.org/10.1038/s41558-018-0359-7>.

1298 Lee, C.-Y., S. J. Camargo, F. Vitart, A. H. Sobel, and M. K. Tippett, 2018: Sub-seasonal tropical  
1299 cyclone genesis prediction and MJO in the S2S dataset. *Wea. Forecasting*, **33**, 967–988,  
1300 <https://doi.org/10.1175/WAF-D-17-0165.1>.

1301 Lee, R., S. Woolnough, A. Charlton-Perez and F. Vitart, 2019: ENSO modulation of MJO  
1302 teleconnection to the North Atlantic & Europe. *Geophys. Res. Lett.*,  
1303 <https://doi.org/10.1029/2019GL084683>.

1304 Lehner, F., A. W. Wood, D. Llewellyn, D. B. Blatchford, A. G. Goodbody, and F. Pappenberger,  
1305 2017: Mitigating the impacts of climate nonstationarity on seasonal streamflow  
1306 predictability in the U.S. Southwest. *Geophys. Res. Lett.*, **44**, 12 208–12 217,  
1307 <https://doi.org/10.1002/2017GL076043>.

1308 Leutbecher, M., and Coauthors, 2017: Stochastic representations of model uncertainties at  
1309 ECMWF: State of the art and future vision. *Quart. J. Roy. Meteor. Soc.*, **143**, 2315–2339,  
1310 <https://doi.org/10.1002/qj.3094>.

1311 Li, B., M. Rodell, B. F. Zaitchik, R. H. Reichle, R. D. Koster, and T. M. van Dam, 2012: Assimilation  
1312 of GRACE terrestrial water storage into a land surface model: Evaluation and potential  
1313 value for drought monitoring in western and central Europe. *J. Hydrol.*, **446–447**, 103–  
1314 115, <https://doi.org/10.1016/j.jhydrol.2012.04.035>.

1315 Li, F., Y. J. Orsolini, N. Keenlyside, M.-L. Shen, F. Counillon, and Y. Wang, 2019: Impact of snow  
1316 initialization in subseasonal-to-seasonal winter forecasts with the Norwegian Climate  
1317 Prediction Model. *J. Geophys. Res. Atmos.*, **124**, 10,033–10,048.  
1318 <https://doi.org/10.1029/2019JD030903>.

1319 Li, H., T. Ilyina, A. Wolfgang, A. Müller, and F. Sienz, 2016: Decadal predictions of the North  
1320 Atlantic CO<sub>2</sub> uptake. *Nat. Commun.*, **7**, 11076, <https://doi.org/10.1038/ncomms11076>.

1321 Li, H. M., and T. Ilyina, 2018: Current and future decadal trends in the oceanic carbon uptake  
1322 are dominated by internal variability. *Geophys. Res. Lett.*, **45**, 916–925,  
1323 <https://doi.org/10.1002/2017GL075370>.

1324 Li, H., T. Ilyina, W. A. Müller, and P. Landschützer., 2019: Predicting the variable ocean carbon  
1325 sink. *Science Advances*, **5**, <https://doi.org/10.1126/sciadv.aav6471>.

1326 Li, S., and A. W. Robertson, 2015: Evaluation of submonthly precipitation forecast skill from  
1327 global ensemble prediction systems. *Mon. Wea. Rev.*, **143**, 2871–2889,  
1328 <https://doi.org/10.1175/MWR-D-14-00277.1>.

1329 Li, X., G. Gollan, R. J. Greatbatch, and R. Lu, 2018: Intraseasonal variation of the East Asian  
1330 summer monsoon associated with the Madden–Julian oscillation. *Atmos. Sci. Lett.*, **19**,  
1331 e794, <https://doi.org/10.1002/asl.794>. Lim, E.-P., and H. H. Hendon, 2017: Causes and  
1332 predictability of the negative Indian Ocean Dipole and its impact on La Niña during 2016.  
1333 *Sci. Rep.*, **7**, 12619, <https://doi.org/10.1038/s41598-017-12674-z>.

1334 Lim, Y., S. Son, and D. Kim, 2018: MJO prediction skill of the subseasonal-to-seasonal prediction  
1335 models. *J. Climate*, **31**, 4075–4094, <https://doi.org/10.1175/JCLI-D-17-0545.1>.

1336 Lim, Y., S.-W. Son, A. G. Marshall, H. H. Hendon, and K.-H. Seo, 2019: Influence of the QBO on  
1337 MJO prediction skill in the subseasonal-to-seasonal prediction models. *Climate Dyn.*,  
1338 <https://doi.org/10.1007/s00382-019-04719-y>.

1339 Lin, H., J. Frederiksen, D. Straus, and C. Stan, 2019: Tropical-Extratropical Interactions and  
1340 Teleconnections. *Sub-Seasonal to Seasonal Prediction*, A. W. Robertson & F. Vitart, Eds.,  
1341 Elsevier, 143-164, <https://doi.org/10.1016/B978-0-12-811714-9.00007-3>.

1342 Liu, X, X. Wang, and A. Kumar, 2018: Multiweek prediction skill assessment of Arctic sea ice  
1343 variability in the CFSv2. *Wea. Forecasting*, **33**, 1453–1476,  
1344 <https://doi.org/10.1175/WAF-D-18-0046.1>.

1345 Lledó, L., V. Torralba, A. Soret, J. Ramon, and F. J. Doblas-Reyes, 2019: Seasonal forecasts of  
1346 wind power generation. *Renewable Energy*, **143**, 91-100,  
1347 <https://doi.org/10.1016/j.renene.2019.04.135>.

1348 Long, C. S., M. Fujiwara, S. Davis, D. M. Mitchell, and C. J. Wright, 2017: Climatology and  
1349 interannual variability of dynamic variables in multiple reanalyses evaluated by the

1350 SPARC Reanalysis Intercomparison Project (S-RIP). *Atmos. Chem. Phys.*, **17**, 14 593–14  
1351 629, <https://doi.org/10.5194/acp-17-14593-2017>.

1352 Lovenduski, N., S. G. Yeager, K. Lindsay, and M. C. Long, 2019: Predicting near-term variability in  
1353 ocean carbon uptake. *Earth Syst. Dyn.*, **10**, 45-57, [https://doi.org/10.5194/esd-10-45-](https://doi.org/10.5194/esd-10-45-2019)  
1354 2019.

1355 Lowe, R., M. García-Díez, J. Ballester, J. Creswick, J.-M. Robine, F. R. Herrmann, and X. Rodó,  
1356 2016: Evaluation of an early-warning system for heat wave-related mortality in Europe:  
1357 Implications for sub-seasonal to seasonal forecasting and climate services. *Int. J. Environ.*  
1358 *Res. Public Health*, **13**, 206, <https://doi.org/10.3390/ijerph13020206>.

1359 Lu, B., A. A. Scaife, N. Dunstone, D. Smith, H.-L. Ren, Y. Liu, and R. Eade, 2017: Skillful seasonal  
1360 predictions of winter precipitation over southern China. *Environ. Res. Lett.*, **12**, 074021,  
1361 <https://doi.org/10.1088/1748-9326/aa739a>.

1362 Luo, J., S. Masson, S. K. Behera, and T. Yamagata, 2008: Extended ENSO predictions using a fully  
1363 coupled ocean–atmosphere model. *J. Climate*, **21**, 84–93,  
1364 <https://doi.org/10.1175/2007JCLI1412.1>.

1365 Luo, J.-J., G. Liu, H. Hendon, O. Alves, and T. Yamagata, 2017: Inter-basin sources for two-year  
1366 predictability of the multi-year La Niña event in 2010–2012. *Sci. Rep.*, **7**, 2276,  
1367 <https://doi.org/10.1038/s41598-017-01479-9>.

1368 Maloney, E. D., and Coauthors, 2019: Process-oriented evaluation of climate and weather  
1369 forecasting Models. *Bull. Amer. Meteor. Soc.*, [https://doi.org/10.1175/BAMS-D-18-](https://doi.org/10.1175/BAMS-D-18-0042.1)  
1370 [0042.1](https://doi.org/10.1175/BAMS-D-18-0042.1).

1371 Manzananas, R., J. M. Gutiérrez, J. Fernández, E. van Meijgaard, S. Calmanti, M. E. Magariño, A. S.  
1372 Cofiño, and S. Herrera, 2018: Dynamical and statistical downscaling of seasonal  
1373 temperature forecasts in Europe: Added value for user applications. *Climate Services*, **9**,  
1374 44-56, <https://doi.org/10.1016/j.cliser.2017.06.004>.

1375 Mariotti, A., P. M. Ruti, and M. Rixen, 2018: Progress in subseasonal to seasonal prediction  
1376 through a joint weather and climate community effort. *NPJ Climate Atmos. Sci.*, **1**, 4,  
1377 <https://doi.org/10.1038/s41612-018-0014-z>.

1378 Mariotti, A. and Coauthors, 2020: Windows of opportunity for skillful forecasts S2S and beyond.  
1379 *Bull. Amer. Meteor. Soc.*, <https://doi.org/10.1175/BAMS-D-18-0326.1>.

1380 Marotzke, J., and Coauthors, 2016: MiKlip—A National Research Project on Decadal Climate  
1381 Prediction. *Bull. Amer. Meteor. Soc.*, **97**, 2379–2394, [https://doi.org/10.1175/BAMS-D-](https://doi.org/10.1175/BAMS-D-15-00184.1)  
1382 [15-00184.1](https://doi.org/10.1175/BAMS-D-15-00184.1).

1383 Marshall, A. G., H. H. Hendon, S.-W. Son, and Y. Lim, 2017: Impact of the quasi-biennial  
1384 oscillation on predictability of the Madden–Julian oscillation. *Climate Dyn.*, **49**, 1365–  
1385 1377, <https://doi.org/10.1007/s00382-016-3392-0>.

1386 Maycock, A. C., and P. Hitchcock, 2015: Do split and displacement sudden stratospheric  
1387 warmings have different annular mode signatures? *Geophys. Res. Lett.*, **42**, 10943–  
1388 10951. <http://doi.org/10.1002/2015GL066754>.

1389 McKinnon, K., A. Rhines, M. Tingly, and P. Huybers, 2016: Long-lead predictions of eastern  
1390 United States hot days from Pacific sea surface temperatures. *Nat. Geosci.*, **9**, 389–394,  
1391 <https://doi.org/10.1038/ngeo2687>.

1392 Meehl, G. A., A. Hu, and H. Teng, 2016: Initialized decadal prediction for transition to positive  
1393 phase of the interdecadal Pacific oscillation. *Nat. Commun.*, **7**, 11718,  
1394 <https://doi.org/10.1038/ncomms11718>.

1395 Menegoz, M., R. Bilbao, O. Bellprat, V. Guemas, and F. J. Doblas-Reyes, 2018: Forecasting the  
1396 climate response to volcanic eruptions: prediction skill related to stratospheric aerosol  
1397 forcing. *Environ. Res. Lett.*, **13**, 064022, <https://doi.org/10.1088/1748-9326/aac4db>.

1398 Misios, S., L. J. Gray, M. F. Knudsen, C. Karoff, H. Schmidt, and J. D. Haigh, 2019: Slowdown of  
1399 the Walker circulation at solar cycle maximum, *Proc. Natl. Acad. Sci. USA*, **116**, 7186-  
1400 7191, <https://doi.org/10.1073/pnas.1815060116>.

1401 Monerie, P.-A., J. Robson, B. Dong, and N. Dunstone, 2018: A role of the Atlantic Ocean in  
1402 predicting summer surface air temperature over North East Asia? *Climate Dyn.*, **51**, 473-  
1403 491, <https://doi.org/10.1007/s00382-017-3935-z>.

1404 Morcrette, C. J., and Coauthors, 2018: Introduction to CAUSES: Description of weather and  
1405 climate models and their near-surface temperature errors in 5 day hindcasts near the  
1406 southern Great Plains *J. Geophys. Res. Atmos.*, **123**, 2655–2683,  
1407 <https://doi.org/10.1002/2017JD027199>.

1408 Mullholland, D. P., P. Laloyaux, K. Haines, and M. Balmaseda, 2015: Origin and impact of  
1409 initialization shocks in coupled atmosphere–ocean forecasts. *Mon. Wea. Rev.*, **143**,  
1410 4631–4644, <https://doi.org/10.1175/MWR-D-15-0076.1>.

1411 Müller, W. A., and Coauthors, 2018: A higher-resolution version of the Max Planck Institute  
1412 Earth System Model (MPI-ESM1.2-HR). *J. Adv. Model. Earth Syst.*, **10**, 1383–1413.  
1413 <https://doi.org/10.1029/2017MS001217>

1414 Muñoz-Sabater, J., H. Lawrence, C. Albergel, P. de Rosnay, L. Isaksen, S. Mecklenburg, Y. Kerr,  
1415 and M. Drusch, 2019: Assimilation of SMOS brightness temperatures in the ECMWF  
1416 Integrated Forecasting System. *Quart. J. Roy. Meteor. Soc.*,  
1417 <https://doi.org/10.1002/qj.3577>.

1418 Neddermann, N. C., W. A. Müller, M. Dobrynin, A. Düsterhus, and J. Baehr, 2019: Seasonal  
1419 predictability of European summer climate re-assessed. *Clim. Dyn.*,  
1420 <https://doi.org/10.1007/s00382-019-04678-4>.

1421 Nie, Y. and Coauthors, 2019 : Stratospheric initial conditions provide seasonal predictability of  
1422 the North Atlantic and Arctic Oscillations. *Environ. Res. Lett.*, **14**, 034006,  
1423 <https://doi.org/10.1088/1748-9326/ab0385>.

1424 Nishimoto, E., and S. Yoden, 2017: Influence of the stratospheric quasi-biennial oscillation on  
1425 the Madden–Julian oscillation during austral summer. *J. Atmos. Sci.*, **74**, 1105–1125,  
1426 <https://doi.org/10.1175/JAS-D-16-0205.1>.

1427 Nnamchi, H. C., J. Li, F. Kucharski, I.-S. Kang, N. S. Keenlyside, P. Chang, and R. Farneti, 2015:  
1428 Thermodynamic controls of the Atlantic Niño. *Nat. Commun.*, **6**, 8895,  
1429 <https://doi.org/10.1038/ncomms9895>.

1430 Nowack, P., P. Braesicke, J. Haigh, N. L. Abraham, J. Pyle, and A. Voulgarakis, 2018. Using  
1431 machine learning to build temperature-based ozone parameterizations for climate  
1432 sensitivity simulations. *Environ. Res. Lett.*, **13**, 104016, [https://doi.org/10.1088/1748-](https://doi.org/10.1088/1748-9326/aae2be)  
1433 [9326/aae2be](https://doi.org/10.1088/1748-9326/aae2be).

1434 O’Reilly, C. H., 2018: Interdecadal variability of the ENSO teleconnection to the wintertime  
1435 North Pacific. *Climate Dyn.*, **51**, 3333-3350, <https://doi.org/10.1007/s00382-018-4081-y>.



1436 O'Reilly, C. H., T. Woollings, L. Zanna, and A. Weisheimer, 2018: The impact of tropical  
1437 precipitation on summertime Euro-Atlantic circulation via a circumglobal wave train. *J.*  
1438 *Climate*, **31**, 6481–6504, <https://doi.org/10.1175/JCLI-D-17-0451.1>.

1439 O'Reilly, C. H., A. Weisheimer, T. Woollings, L. Gray, and D. MacLeod, 2019: The importance of  
1440 stratospheric initial conditions for winter North Atlantic Oscillation predictability and  
1441 implications for the signal-to-noise paradox. *Quart. J. Roy. Meteor. Soc.*, **145**,  
1442 <https://doi.org/10.1002/qj.3413>.

1443 Orsolini, Y. J., R. Senan, G. Balsamo, F. J. Doblas-Reyes, F. Vitart, A. Weisheimer, A. Carrasco,  
1444 and R. E. Benestad, 2013: Impact of snow initialization on sub-seasonal forecasts. *Clim.*  
1445 *Dyn.*, **41**, 1969–1982, <https://doi.org/10.1007/s00382-013-1782-0>.

1446 Pasternack, A., J. Bhend, M. A. Liniger, H. W. Rust, W. A. Müller, and U. Ulbrich, 2018:  
1447 Parametric decadal climate forecast recalibration (DeFoReSt 1.0), *Geosci. Model Dev.*,  
1448 **11**, 351-368, <https://doi.org/10.5194/gmd-11-351-2018>.

1449 Patricola, C. M., S. J. Camargo, P. J. Klotzbach, R. Saravanan, and P. Chang, 2018: The influence  
1450 of ENSO flavors on western North Pacific tropical cyclone activity. *J. Climate*, **31**, 5395–  
1451 5416, <https://doi.org/10.1175/JCLI-D-17-0678.1>.

1452 Pegion, K., and Coauthors, 2019: The Subseasonal Experiment (SubX): A multi-model  
1453 subseasonal prediction experiment. *Bull. Am. Met. Soc.*, [https://doi.org/10.1175/BAMS-](https://doi.org/10.1175/BAMS-D-18-0270.1)  
1454 [D-18-0270.1](https://doi.org/10.1175/BAMS-D-18-0270.1).

1455 Penny, S. G., and T. M. Hamill, 2017: Coupled data assimilation for integrated Earth system  
1456 analysis and prediction. *Bull. Amer. Meteor. Soc.*, **98**, ES169–ES172,  
1457 <https://doi.org/10.1175/BAMS-D-17-0036.1>.

1458 Penny, S.G., and Coauthors, 2017: Coupled Data Assimilation for Integrated Earth System  
1459 Analysis and Prediction: Goals, Challenges and Recommendations. Technical Report.  
1460 WWRP 2017-3, World Meteorological Organization (WMO).

1461 Penny, S. G., E. Bach, K. Bhargava, C.-C. Chang, C. Da, L. Sun, and T. Yoshida, 2019: Strongly  
1462 coupled data assimilation in multiscale media: Experiments using a quasi-geostrophic  
1463 coupled model. *J. Adv. Model. Earth Syst.*, **11**, 1803–1829,  
1464 <https://doi.org/10.1029/2019MS001652>.

1465 Polkova, I., and Coauthors, 2019: Initialization and ensemble generation for decadal climate  
1466 predictions: A comparison of different methods. *J. Adv. Model. Earth Syst.*, **11**, 149–172.  
1467 <https://doi.org/10.1029/2018MS001439>.

1468 Prodhomme, C., F. Doblas-Reyes, O. Bellprat, and E. Dutra, 2016a: Impact of land-surface  
1469 initialization on sub-seasonal to seasonal forecasts over Europe. *Climate Dyn.*, **47**, 919–  
1470 935, <https://doi.org/10.1007/s00382-015-2879-4>.

1471 Prodhomme, C., L. Batté, F. Massonnet, P. Davini, O. Bellprat, V. Guemas, and F. Doblas-Reyes,  
1472 2016b: Benefits of increasing the model resolution for the seasonal forecast quality in  
1473 EC-Earth. *J. Climate*, **29**, 9141–9162, <https://doi.org/10.1175/JCLI-D-16-01117.1>.

1474 Robertson, A. W., S. J. Camargo, A. Sobel, F. Vitart, and S. Wang, 2018: Summary of workshop  
1475 on sub-seasonal to seasonal predictability of extreme weather and climate. *NPJ Climate*  
1476 *Atmos. Sci.*, **1**, 20178, <https://doi.org/10.1038/s41612-017-0009-1>.

1477 Robson, J., P. Ortega, and R. Sutton, 2016: A reversal of climatic trends in the North Atlantic  
1478 since 2005. *Nat. Geosci.*, **9**, 513–517, <https://doi.org/10.1038/ngeo2727>.

1479 Ruprich-Robert, Y., R. Msadek, F. Castruccio, S. Yeager, T. Delworth, and G. Danabasoglu, 2017:  
1480 Assessing the climate impacts of the observed Atlantic multidecadal variability using the  
1481 GFDL CM2.1 and NCAR CESM1 global coupled models. *J. Climate*, **30**, 2785–2810,  
1482 <https://doi.org/10.1175/JCLI-D-16-0127.1>.

1483 Ruprich-Robert, Y., T. Delworth, R. Msadek, F. Castruccio, S. Yeager, and G. Danabasoglu, 2018:  
1484 Impacts of the Atlantic multidecadal variability on North American summer climate and  
1485 heat waves. *J. Climate*, **31**, 3679–3700, <https://doi.org/10.1175/JCLI-D-17-0270.1>.

1486 Sanchez-Gomez, E., C. Cassou, Y. Ruprich-Robert, E. Fernandez, and L. Terray, 2016: Drift  
1487 dynamics in a coupled model initialized for decadal forecasts. *Climate Dyn.*, **46**, 1819–  
1488 1840, <https://doi.org/10.1007/s00382-015-2678-y>.

1489 Santanello, J. A., and Coauthors, 2018: Land-Atmosphere Interactions: The LoCo Perspective.  
1490 *Bull. Amer. Meteor. Soc.*, **99**, 1253–1272, <https://doi.org/10.1175/BAMS-D-17-0001.1>.

1491 Saravanan, R., and P. Chang, 2019: Midlatitude mesoscale ocean-atmosphere interaction and its  
1492 relevance to S2S prediction. *Sub-Seasonal to Seasonal Prediction*, A. W. Robertson & F.  
1493 Vitart, Eds., Elsevier, 183– 200, <https://doi.org/10.1016/B978-0-12-811714-9.00009-7>.

1494 Scaife, A. A., and Coauthors, 2014a: Predictability of the quasi-biennial oscillation and its  
1495 northern winter teleconnection on seasonal to decadal timescales. *Geophys. Res. Lett.*,  
1496 **41**, 1752–1758, <https://doi.org/10.1002/2013GL059160>.

1497 Scaife, A., and Coauthors, 2014b: Skillful long-range predictions of European and North  
1498 American winters. *Geophys. Res. Lett.*, **41**, 2514–2519,  
1499 <https://doi.org/10.1002/2014GL059637>.

1500 Scaife, A. A., and Coauthors, 2017: Tropical rainfall, Rossby waves and regional winter climate  
1501 predictions. *Quart. J. Roy. Meteor. Soc.*, **143**, 1–11, <https://doi.org/10.1002/qj.2910>.

1502 Scaife, A. A., and D. Smith, 2018: A signal to noise paradox in climate science. *npj Clim. Atmos.*  
1503 *Sci.*, **1**, 28, <https://doi.org/10.1038/s41612-018-0038-4>.

1504 Scaife, A. A., and Coauthors, 2019: Does increased atmospheric resolution improve seasonal  
1505 climate predictions? *Atmos. Sci. Lett.*, **20**, e922, <https://doi.org/10.1002/asl.922>.

1506 Schuster, M., and Coauthors, 2019: Improvement in the decadal prediction skill of the northern  
1507 hemisphere extra-tropical winter circulation through increased model resolution, *Earth*  
1508 *Syst. Dynam. Discuss.*, <https://doi.org/10.5194/esd-2019-18>.

1509 Sheen, K. L., D. M. Smith, N. J. Dunstone, R. Eade, D. P. Rowell, and M. Vellinga, 2017: Skilful  
1510 prediction of Sahel summer rainfall on inter-annual and multi-year timescales. *Nat.*  
1511 *Commun.*, **8**, 14966, <https://doi.org/10.1038/ncomms14966>.

1512 Shen, M.-L., N. Keenlyside, F. Selten, W. Wiegner, and G. S. Duane, 2016: Dynamically  
1513 combining climate models to “supermodel” the tropical Pacific. *Geophys. Res. Lett.*, **43**,  
1514 359–366, <https://doi.org/10.1002/2015GL066562>.

1515 Shonk, J. K., E. Guilyardi, T. Toniazzo, S. J. Woolnough, and T. Stockdale, 2018: Identifying causes  
1516 of western Pacific ITCZ drift in ECMWF System 4 hindcasts. *Climate Dyn.*, **50**, 939–954,  
1517 <https://doi.org/10.1007/s00382-017-3650-9>.

1518 Shonk, J. K. P., T. D. Demissie, and T. Toniazzo, 2019: A double ITCZ phenomenology of wind  
1519 errors in the equatorial Atlantic in seasonal forecasts with ECMWF models. *Atmos.*  
1520 *Chem. Phys.*, **19**, 11383–11399, <https://doi.org/10.5194/acp-19-11383-2019>.

1521 Sigmond, M., J. F. Scinocca, V. V. Kharin, and T. G. Shepherd, 2013: Enhanced seasonal forecast  
1522 skill following stratospheric sudden warmings. *Nat. Geosci.*, **6**, 98–102,  
1523 doi:<https://doi.org/10.1038/ngeo1698>.

1524 Simpson, I. R., P. Hitchcock, R. Seager, Y. Wu, and P. Callaghan, 2018: The downward influence  
1525 of uncertainty in the Northern Hemisphere stratospheric polar vortex response to  
1526 climate change. *J. Climate*, **31**, 6371– 6391. <https://doi.org/10.1175/JCLI-D-18-0041.1>.

1527 Smith, D. M., and Coauthors, 2016: Role of the volcanic and anthropogenic aerosols in the  
1528 recent global surface warming slowdown. *Nat. Climate Change*, **6**, 936–940,  
1529 <https://doi.org/10.1038/nclimate3058>.

1530 Smith, D. M., and Coauthors, 2019: Robust skill of decadal climate predictions, *npj Clim. Atmos.*  
1531 *Sci.*, **2**, 13, <https://doi.org/10.1038/s41612-019-0071-y>.

1532 Sospedra-Alfonso, R., L. Mudryk, W. J. Merryfield and C. Derksen, 2016a: Representation of  
1533 snow in the Canadian Seasonal to Interannual Prediction System: Part I. Initialization. *J.*  
1534 *Hydrometeorology*, **17**, 1467-1488, <https://doi.org/10.1175/JHM-D-14-0223.1>.

1535 Sospedra-Alfonso, R., W. J. Merryfield and V. V. Kharin, 2016b: Representation of snow in the  
1536 Canadian Seasonal to Interannual Prediction System: Part II. Potential predictability and  
1537 hindcast skill. *J. Hydrometeorology*, **17**, 2511-2535, [https://doi.org/10.1175/JHM-D-16-](https://doi.org/10.1175/JHM-D-16-0027.1)  
1538 [0027.1](https://doi.org/10.1175/JHM-D-16-0027.1).

1539 Stan, C., and D. M. Straus, 2019: The impact of cloud representation on the sub-seasonal  
1540 forecasts of atmospheric teleconnections and preferred circulation regimes in the  
1541 northern hemisphere. *Atmosphere-Ocean*, **57**, 233-248,  
1542 <https://doi.org/10.1080/07055900.2019.1590178>.

1543 Stephenson, S. R., and R. Pincus, 2018: Challenges of sea-ice prediction for Arctic marine policy  
1544 and planning. *J. Borderlands Studies*, **33**, 255– 272,  
1545 <https://doi.org/10.1080/08865655.2017.1294494>.

1546 Strommen K., and T. N. Palmer, 2019: Signal and noise in regime systems: A hypothesis on the  
1547 predictability of the North Atlantic Oscillation. *Quart. J. Roy. Meteor. Soc.*, **145**, 147–163,  
1548 <https://doi.org/10.1002/qj.3414>.

1549 Stone, K. A., S. Solomon, D. E. Kinnison, C. F. Baggett, and Elizabeth A. Barnes, 2019: Prediction  
1550 of Northern Hemisphere regional surface temperatures using stratospheric ozone  
1551 information. *J. Geophys. Res.*, **124**, 5922-5933, <https://doi.org/10.1029/2018JD029626>.

1552 Swingedouw, D., J. Mignot, P. Ortega, M. Khodri, M. Menegoz, C. Cassou, and V. Hanquiez,  
1553 2017: Impact of explosive volcanic eruptions on the main climate variability modes.  
1554 *Global Planet. Change*, **150**, 24–45, <https://doi.org/10.1016/j.gloplacha.2017.01.006>.

1555 Strazzo, S., D. C. Collins, A. Schepen, Q. J. Wang, E. Becker, and L. Jia, 2019: Application of a  
1556 hybrid statistical-dynamical system to seasonal prediction of North American  
1557 temperature and precipitation. *Mon. Wea. Rev.*, **147**, 607-625,  
1558 <https://doi.org/10.1175/MWR-D-18-0156.1>.

1559 Taguchi, M., 2018: Comparison of Subseasonal-to-Seasonal Model Forecasts for Major  
1560 Stratospheric Sudden Warmings. *J. Geophys. Res.*, **123**, 10,231-10,247,  
1561 <https://doi.org/10.1029/2018JD028755>.

1562 Takahashi, C., and M. Watanabe, 2016: Pacific trade winds accelerated by aerosol forcing over  
1563 the past two decades. *Nat. Climate Change*, **6**, 768–772,  
1564 <https://doi.org/10.1038/nclimate2996>.

1565 Takaya, Y., 2019: Forecast System Design, Configuration, and Complexity. *Sub-Seasonal to*  
1566 *Seasonal Prediction*, A. W. Robertson & F. Vitart, Eds., Elsevier, 93-117,  
1567 <https://doi.org/10.1016/B978-0-12-811714-9.00012-7>.

1568 Teng, H., G. Branstator, A. B. Tawfik, and P. Callaghan, 2019: Circumglobal response to  
1569 prescribed soil moisture over North America. *J. Climate*, **32**, 4525– 4545.  
1570 <https://doi.org/10.1175/JCLI-D-18-0823.1>

1571 Tommasi, D. and Coauthors, 2017: Managing living marine resources in a dynamic environment:  
1572 The role of seasonal to decadal climate forecasts. *Prog. Oceanogr.*, **152**, 15–49,  
1573 <https://doi.org/10.1016/j.pocean.2016.12.011>.

1574 Toniazzo, T., and S. Koseki, 2018: A methodology for anomaly coupling in climate simulation. *J.*  
1575 *Adv. Model. Earth Syst.*, **10**, 2061–2079, <https://doi.org/10.1029/2018MS001288>.

1576 Toure, A. M., R. H. Reichle, B. A. Forman, A. Getirana, and G. J. M. De Lannoy, 2018.  
1577 Assimilation of MODIS snow cover fraction observations into the NASA Catchment land  
1578 surface model. *Remote Sensing*, **10**, 316. <https://doi.org/10.3390/rs10020316>.

1579 Towler, E., D. PaiMazumder, and J. Done, 2018: Toward the application of decadal climate  
1580 predictions. *J. App. Meteorol. Climatol.*, **57**, 555-568, [https://doi.org/10.1175/JAMC-D-](https://doi.org/10.1175/JAMC-D-17-0113.1)  
1581 [17-0113.1](https://doi.org/10.1175/JAMC-D-17-0113.1).

1582 Tripathi, O. P., and Coauthors, 2015: The predictability of the extratropical stratosphere on  
1583 monthly time-scales and its impact on the skill of tropospheric forecasts. *Quart. J. Roy.*  
1584 *Meteor. Soc.*, **141**, 987–1003, <https://doi.org/10.1002/qj.2432>.

1585 Turco, M., R. Marcos-Matamorosa, X. Castro, E. Canyameras, and M. C. Llasat, 2019: Seasonal  
1586 prediction of climate-driven fire risk for decision-making and operational applications in

1587 a Mediterranean region. *Sci. Total Environ.*, **676**, 577-583,  
1588 <https://doi.org/10.1016/j.scitotenv.2019.04.296>.

1589 Uotila, P., and Coauthors, 2019: An assessment of ten ocean reanalyses in the polar regions.  
1590 *Climate Dyn.*, **52**, 1613–1650, <https://doi.org/10.1007/s00382-018-4242-z>.

1591 Vigaud, N., A. Robertson, and M. Tippett, 2017: Multimodel ensembling of subseasonal  
1592 precipitation forecasts over North America. *Mon. Wea. Rev.*, **145**, 3913–3928,  
1593 <https://doi.org/10.1175/MWR-D-17-0092.1>.

1594 Vitart, F., 2017: Madden–Julian oscillation prediction and teleconnections in the S2S database.  
1595 *Quart. J. Roy. Meteor. Soc.*, **143**, 2210–2220, <https://doi.org/10.1002/qj.3079>.

1596 Vitart, F., and M. Balmaseda, 2017: Impact of sea surface temperature biases on extended-  
1597 range forecasts. ECMWF Technical Memorandum 830.

1598 Vitart, F., and Coauthors, 2017: The Subseasonal to Seasonal (S2S) Prediction project database.  
1599 *Bull. Amer. Meteor. Soc.*, **98**, 163–173, <https://doi.org/10.1175/BAMS-D-16-0017.1>.

1600 Vitart, F., and A. W. Robertson, 2018: The sub-seasonal to seasonal prediction project (S2S) and  
1601 the prediction of extreme events. *npj Climate Atmos. Sci.*, **1**, 3,  
1602 <https://doi.org/10.1038/s41612-018-0013-0>.

1603 Vitart, F., and A. Robertson, 2019: Introduction: Why Sub-seasonal to Seasonal Prediction (S2S)?  
1604 *Sub-Seasonal to Seasonal Prediction*, A. W. Robertson & F. Vitart, Eds., Elsevier, 3–15,  
1605 <https://doi.org/10.1016/B978-0-12-811714-9.00001-2>.

1606 Voltaire, A., and Coauthors, 2019 : Role of wind stress in driving SST biases in the Tropical  
1607 Atlantic. *Climate Dyn.*, **53**, 3481–3504, <https://doi.org/10.1007/s00382-019-04717-0>.



1608 Volpi, D., V. Guemas, and F. J. Doblas-Reyes, 2017: Comparison of full field and anomaly  
1609 initialisation for decadal climate prediction: Towards an optimal consistency between  
1610 the ocean and sea-ice anomaly initialisation state. *Climate Dyn.*, **49**, 1181–1195,  
1611 <https://doi.org/10.1007/s00382-016-3373-3>.

1612 Wang, H. L., S. D. Schubert, R. D. Koster, and Y. Chang, 2019: Phase locking of the boreal  
1613 summer atmospheric response to dry land surface anomalies in the Northern  
1614 Hemisphere. *J. Climate*, **32**, 1081–1099, <https://doi.org/10.1175/JCLI-D-18-0240.1>.

1615 Wang, T., D. Guo, Y. Gao, H. Wang, F. Zheng, Y. Zhu, J. Miao, and Y. Hu, 2018: Modulation of  
1616 ENSO evolution by strong tropical volcanic eruptions. *Climate Dyn.*, **51**, 2433–2453,  
1617 <https://doi.org/10.1007/s00382-017-4021-2>.

1618 Wei, J., and P. A. Dirmeyer, 2019: Sensitivity of land precipitation to surface evapotranspiration:  
1619 a nonlocal perspective based on water vapor transport. *Geophys. Res. Lett.*,  
1620 <https://doi.org/10.1029/2019GL085613>.

1621 Weisheimer, A., and T. Palmer, 2014: On the reliability of seasonal climate forecasts. *J. Roy. Soc.*  
1622 *Interface*, **11**, 20131162, <https://doi.org/10.1098/rsif.2013.1162>.

1623 Weisheimer, A., D. Decremmer, D. MacLeod, C. O'Reilly, T. N. Stockdale, S. Johnson, and T. N.  
1624 Palmer, 2019: How confident are predictability estimates of the winter North Atlantic  
1625 Oscillation? *Quart. J. Roy. Meteor. Soc.*, **145**, 1-20, <https://doi.org/10.1002/qj.3446>.

1626 Weiss, M., and Coauthors, 2014: Contribution of dynamic vegetation phenology to decadal  
1627 climate predictability. *J. Climate*, **27**, 8563–8577, [https://doi.org/10.1175/JCLI-D-13-](https://doi.org/10.1175/JCLI-D-13-00684.1)  
1628 [00684.1](https://doi.org/10.1175/JCLI-D-13-00684.1).

1629 White, C. J., and Coauthors, 2017: Potential applications of subseasonal-to-seasonal (S2S)  
1630 predictions. *Meteor. Appl.*, **24**, 315–325, <https://doi.org/10.1002/met.1654>.

1631 Widlansky, M., and Coauthors, 2017: Multi-model ensemble sea level forecasts for tropical  
1632 Pacific islands. *J. Appl. Meteor. Climatol.*, **56**, 849– 862. <https://doi.org/10.1175/JAMC->  
1633 [D-16-0284.1](https://doi.org/10.1175/JAMC-D-16-0284.1).

1634 Williams, I. N., Y. Lu, L. M. Kueppers, W. J. Riley, S. Biraud, J. E. Bagley, and M. S. Torn, 2016:  
1635 Land–atmosphere coupling and climate prediction over the US Southern Great Plains. *J.*  
1636 *Geophys. Res. Atmos.*, **121**, 12 125–12 144, <https://doi.org/10.1002/2016JD025223>.

1637 Woolnough, S. J., 2019: The Madden-Julian Oscillation. *Sub-Seasonal to Seasonal Prediction*, A.  
1638 W. Robertson & F. Vitart, Eds., Elsevier, 93-117, <https://doi.org/10.1016/B978-0-12->  
1639 [811714-9.00005-X](https://doi.org/10.1016/B978-0-12-811714-9.00005-X).

1640 World Meteorological Organization, 2018: Manual on the Global Data-processing and  
1641 Forecasting System: Annex IV to the WMO Technical Regulations (2018 update). WMO-  
1642 485, 119 pp., [https://library.wmo.int/doc\\_num.php?explnum\\_id=5839](https://library.wmo.int/doc_num.php?explnum_id=5839).

1643 Xue, Y. K., and Coauthors, 2018: Spring land surface and subsurface temperature anomalies and  
1644 subsequent downstream late spring-summer droughts/floods in North America and East  
1645 Asia. *J. Geophys. Res. Atmos.*, **129**, 5001–5019, <https://doi.org/10.1029/2017JD028246>.

1646 Yang, S., Z. Li, J.-Y. Yu, X. Hu, W. Dong, and S. He, 2018: El Niño–Southern oscillation and its  
1647 impact in the changing climate. *National Science Review*, **5**, 840–857.  
1648 <https://doi.org/10.1093/nsr/nwy046>.

1649 Yang, X., and T. DelSole, 2012: Systematic comparison of ENSO teleconnection patterns  
1650 between models and observations. *J. Climate*, **25**, 425–446,  
1651 <https://doi.org/10.1175/JCLI-D-11-00175.1>.

1652 Yang, Z., J. Zhang, and L. Wu, 2019: Spring soil temperature as a predictor of summer  
1653 heatwaves over northwestern China. *Atmos. Sci. Lett.*, **20**, e887,  
1654 <https://doi.org/10.1002/asl.887>.

1655 Yeager, S., and J. I. Robson, 2017: Recent progress in understanding and predicting Atlantic  
1656 decadal climate variability. *Curr. Climate Change Rep.*, **3**, 112–127,  
1657 <https://doi.org/10.1007/s40641-017-0064-z>.

1658 Yeager, S. G., and Coauthors, 2018: Predicting near-term changes in the Earth System: A large  
1659 ensemble of initialized decadal prediction simulations using the Community Earth System  
1660 Model. *Bull. Amer. Meteor. Soc.*, **99**, 1867–1886, [https://doi.org/10.1175/BAMS-D-17-](https://doi.org/10.1175/BAMS-D-17-0098.1)  
1661 [0098.1](https://doi.org/10.1175/BAMS-D-17-0098.1).

1662 Yeh, S.-W., and Coauthors, 2018: ENSO atmospheric teleconnections and their response to  
1663 greenhouse gas forcing. *Rev. Geophys.*, **56**, 185–206,  
1664 <https://doi.org/10.1002/2017RG000568>.

1665 Yoo, C., S. Park, D. Kim, J.-H. Yoon, and H.-M. Kim, 2015: Boreal winter MJO teleconnection in the  
1666 Community Atmosphere Model version 5 with the unified convection parameterization.  
1667 *J. Climate*, **28**, 8135–8150, <https://doi.org/10.1175/JCLI-D-15-0022.1>.

1668 Yoo, C., and S.-W. Son, 2016: Modulation of the boreal wintertime Madden-Julian oscillation by  
1669 the stratospheric quasi-biennial oscillation. *Geophys. Res. Lett.*, **43**, 1392–1398,  
1670 <https://doi.org/10.1002/2016GL067762>.

1671 Yuan, X., M. R. Kaplan, and M. A. Cane, 2018: The Interconnected Global Climate System—A  
1672 Review of Tropical–Polar Teleconnections. *J. Climate*, **31**, 5765–5792,  
1673 <https://doi.org/10.1175/JCLI-D-16-0637.1>.

1674 Yun, K. S., and A. Timmermann, 2018: Decadal monsoon–ENSO relationships reexamined.  
1675 *Geophys. Res. Lett.*, **45**, 2014–2021, <https://doi.org/10.1002/2017GL076912>.

1676 Zampieri, L., H. F. Goessling and T. Jung, 2018: Bright prospects for Arctic sea ice prediction on  
1677 subseasonal time scales. *Geophys. Res. Lett.*, **45**, 9731– 9738,  
1678 <https://doi.org/10.1029/2018GL079394>.

1679 Zhang, W. and B. Kirtman, 2019: Understanding the signal-to-noise paradox with a simple  
1680 Markov model. *Geophys. Res. Lett.*, <https://doi.org/10.1029/2019GL085159>.

1681 Zhang, L., T. L. Delworth, W. Cooke, and X. Yang, 2019: Natural variability of Southern Ocean  
1682 convection as a driver of observed climate trends. *Nat. Climate Change*, **9**, 59–65,  
1683 <https://doi.org/10.1038/s41558-018-0350-3>.

1684 Zhang, Y., T. Zou, and Y. Xue, 2019: An Arctic-Tibetan Connection on Subseasonal to Seasonal  
1685 Time Scale. *Geophys. Res. Lett.*, **46**, 2790–2799, <https://doi.org/10.1029/2018GL081476>.

1686 Zhao, C., H.-L. Ren, R. Eade, Y. Wu, J. Wu, and C. MacLachlan, 2019: MJO modulation and its  
1687 ability to predict boreal summer tropical cyclone genesis over the northwest Pacific in  
1688 Met Office Hadley Centre and Beijing Climate Center seasonal prediction systems.  
1689 *Quart. J. Roy. Meteor. Soc.*, **145**, 1089– 1101. <https://doi.org/10.1002/qj.3478>.

1690 Zhu, J., and Coauthors, 2015: ENSO prediction in Project Minerva: Sensitivity to atmospheric  
1691 horizontal resolution and ensemble size. *J. Climate*, **28**, 2080–2095,  
1692 <https://doi.org/10.1175/JCLI-D-14-00302.1>.

1693 **SIDEBAR 1:**

1694 **Hindcast and forecast quality assessment (or, “the unexamined life is not worth living”).**

1695 Besides helping to inform decision making, the careful assessment of forecast quality is critical  
1696 to guiding forecasting improvements, but has many and varied considerations. Simply  
1697 answering the question “is this forecast better than that one?” is complicated, as the  
1698 appropriate skill metric or means for comparison is not always obvious. Some recent studies  
1699 have focused on newer statistical methods for comparing one forecast to another. One  
1700 relatively simple approach is the random walk test (DelSole and Tippett 2016), illustrated in Fig.  
1701 SB1. This method is applicable to a wide range of measures such as a score based on the earth  
1702 mover’s distance metric (Düsterhus 2019), while also being robust and fair in its discrimination.

1703

1704 The utility of forecast assessment can be illustrated through two very different applications of  
1705 seasonal forecasts: sea-ice and hurricanes. The assessment of seasonal sea ice forecasts is  
1706 complicated by the low quality of sea-ice observations, but nevertheless reveals that initializing  
1707 sea-ice thickness using observational data sets generally improves the prediction of Arctic sea-  
1708 ice extent and edges (Blockley et al. 2018). Comparison of multi-annual forecasts of Atlantic  
1709 hurricane activity obtained by direct tracking of storms in decadal hindcasts and through a  
1710 hybrid approach combining predicted SSTs and observed statistical relations finds that each  
1711 approach is skillful, especially hybrid forecasts based on a SST index for AMV (Caron et al.  
1712 2018).

1713

1714 A robust assessment of model performance should include the model's simulation of climate  
1715 modes and teleconnection patterns such as ENSO, MJO and NAO, since they are major sources  
1716 of predictability and errors representing their patterns or strength (e.g., Yang and DelSole  
1717 2012; Vitart 2017) can degrade skill in affected regions (Gleixner et al. 2017; Lu et al. 2017). In  
1718 cases where modeled teleconnection patterns are imperfect, forecast skill may be improved by  
1719 means of statistical methods that use model forecasts of relevant climate modes such as ENSO  
1720 as predictors (e.g., Strazzo et al. 2019). It remains desirable, however, for models to improve so  
1721 that their simulated teleconnection patterns are sufficiently realistic that such corrections are  
1722 not needed.

1723

1724 **SIDEBAR 2:**

1725 **Frontiers in Earth system prediction.**

1726 New frontiers in S2D prediction have been enabled by Earth system models (ESMs, Flato 2011)  
1727 that represent the carbon and other biogeochemical cycles in addition to the physical climate  
1728 system. These frontiers include prediction of ocean and land carbon sinks and biogeochemistry  
1729 and their important contribution to global carbon storage, as well as ecosystem services. The  
1730 world's oceans are a fundamental regulator of global carbon storage and variability. The  
1731 strength of ocean carbon uptake, together with uptake of carbon by the land, determines the  
1732 fraction of anthropogenic emissions remaining in the atmosphere, and hence modulates  
1733 present and future warming. Observed global mean ocean carbon uptake shows variability on  
1734 decadal time scales that can be represented by ESMs in which physical climate variables are  
1735 assimilated (H. Li et al. 2019).

1736

1737 ESM simulations indicate that internal variability of the ocean carbon uptake on decadal  
1738 timescales is as large as the forced climate change trend (Li and Ilyina 2018), pointing to the  
1739 potential importance and utility of decadal carbon cycle predictions. Decadal predictions from a  
1740 number of ESMs are assessing the predictability of the ocean and land carbon sinks and other  
1741 ocean tracers such as dissolved oxygen. These forecasts are part of the Decadal Climate  
1742 Prediction Project (Boer et al. 2016) and international programs such as the World Climate  
1743 Research Programme's Grand Challenge on Carbon Feedbacks (Ilyina and Friedlingstein 2016).  
1744 Initial results based on individual models have demonstrated potential predictive skill, assessed  
1745 through verification against the assimilating reconstructions that provide initial conditions, for  
1746 ocean carbon uptake in certain regions such as the North Atlantic reaching up to 7 or more  
1747 years (Li et al. 2016; Lovenduski et al. 2019), and skill in predicting actual variations estimated  
1748 from observations (Fig. SB2) has been demonstrated (Li et al. 2019).

1749 ESM-based studies also point to the drivers of this predictability. Air-sea CO<sub>2</sub> flux mainly varies  
1750 due to pCO<sub>2</sub> changes in the ocean. While thermal influences on pCO<sub>2</sub> play a role in shorter term  
1751 predictability, predictability beyond 3 years is maintained mainly by nonthermal influences of  
1752 ocean circulation and biological modification of surface dissolved inorganic carbon and  
1753 alkalinity (Li et al. 2019; Lovenduski et al. 2019).

1754

1755 Investigations in progress are finding potential for multi-annual prediction of additional  
1756 biogeochemical fields such as net primary productivity and interior dissolved oxygen  
1757 concentrations. In addition, potential predictability and skill for terrestrial carbon uptake have

1758 also begun to be assessed, with promising initial results (N. Lovenduski 2019, personal  
1759 communication). These examples demonstrate that skillful multi-year prediction is likely  
1760 achievable for biogeochemical and ecological Earth system components, and open prospects  
1761 for the utilization of such information although significant challenges including the paucity of  
1762 long term observational data for initialization and verification will need to be overcome.

1763

1764

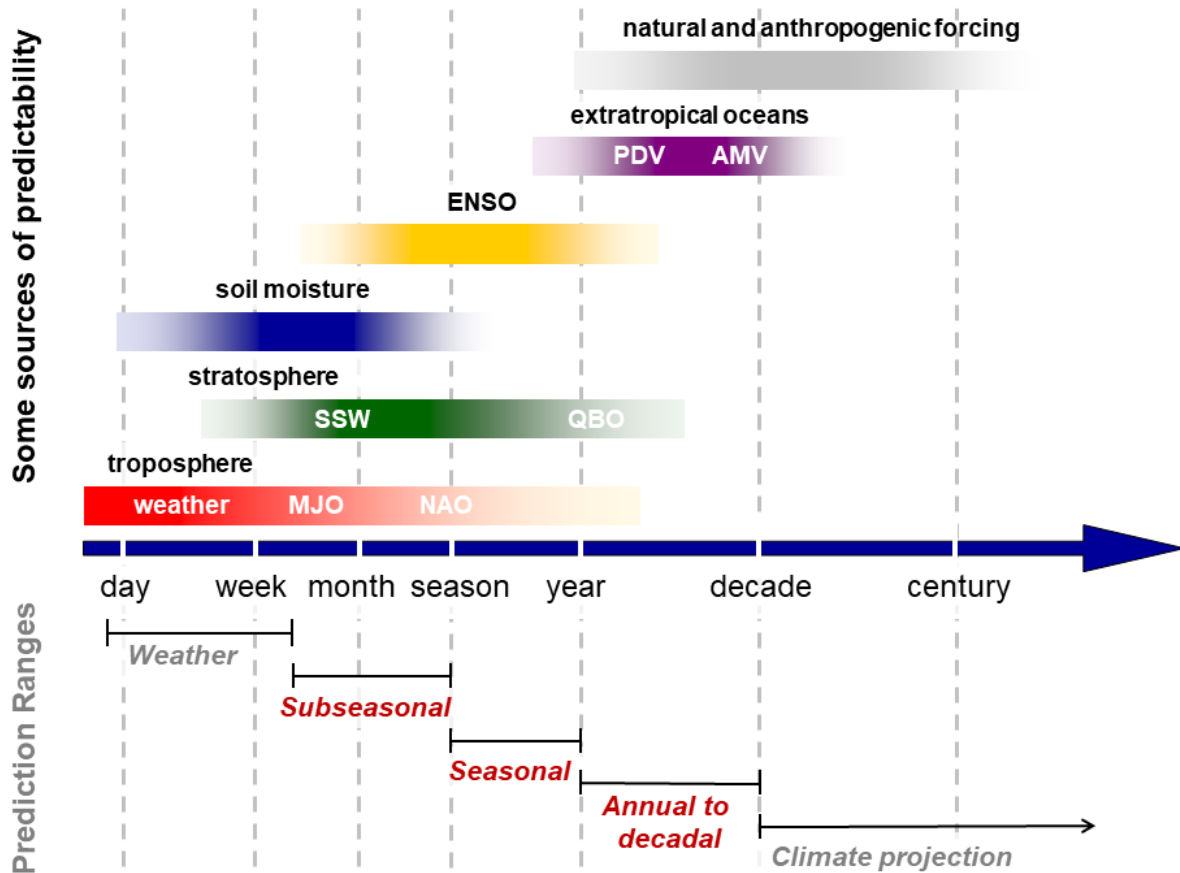
1765

1766

1767

1768





1769

1770

1771 **Fig. 1.** Schematic depiction of temporal ranges and sources of predictability for weather and climate

1772 prediction. The subseasonal range encompasses the S2S time scales, and the seasonal and annual-to-

1773 decadal ranges the S2D time scales, that are considered in this paper. Longer multi-decadal and

1774 centennial ranges derive predictability mainly from forcing scenarios rather than initial conditions, and

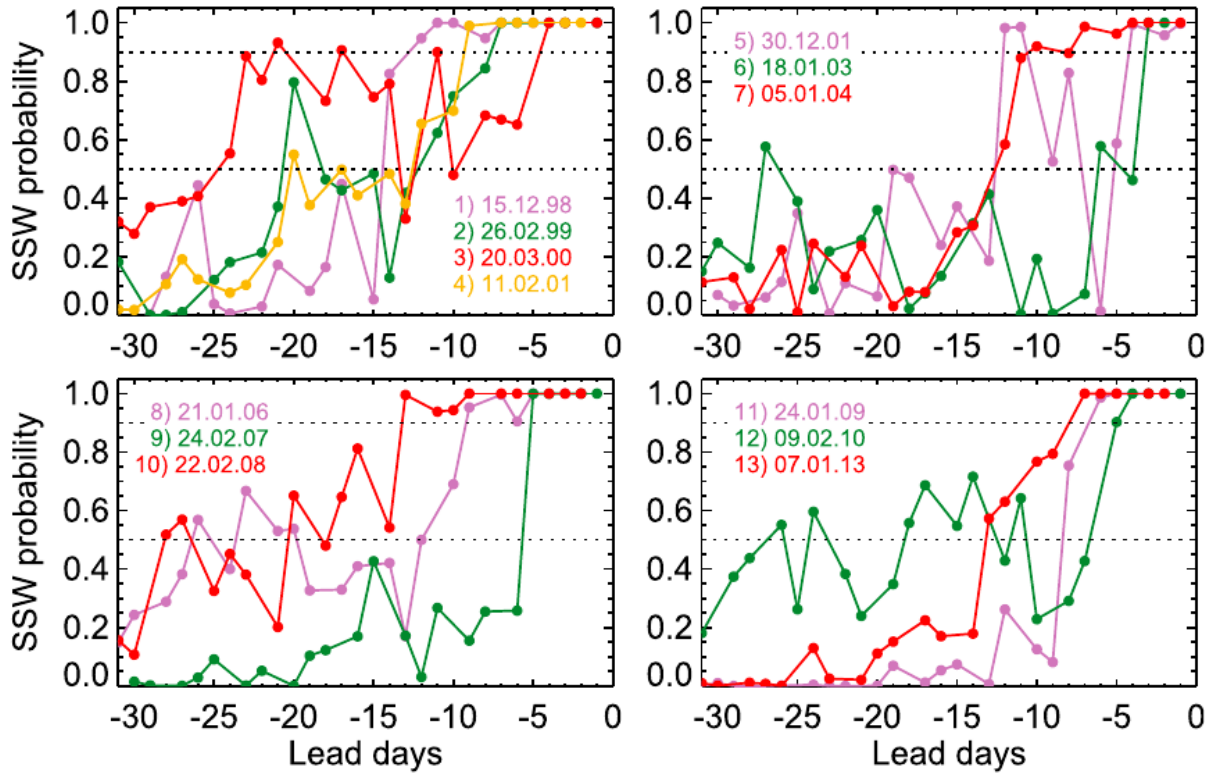
1775 are typically represented through climate projections originating from historical simulations begun in

1776 preindustrial times rather than predictions initialized from more recent observation-based climate

1777 states. Some important sources of predictability and approximate time scales over which they are most

1778 influential on surface climate are indicated in the upper portion of the figure; acronyms are defined and

1779 associated phenomena are discussed in the main text.



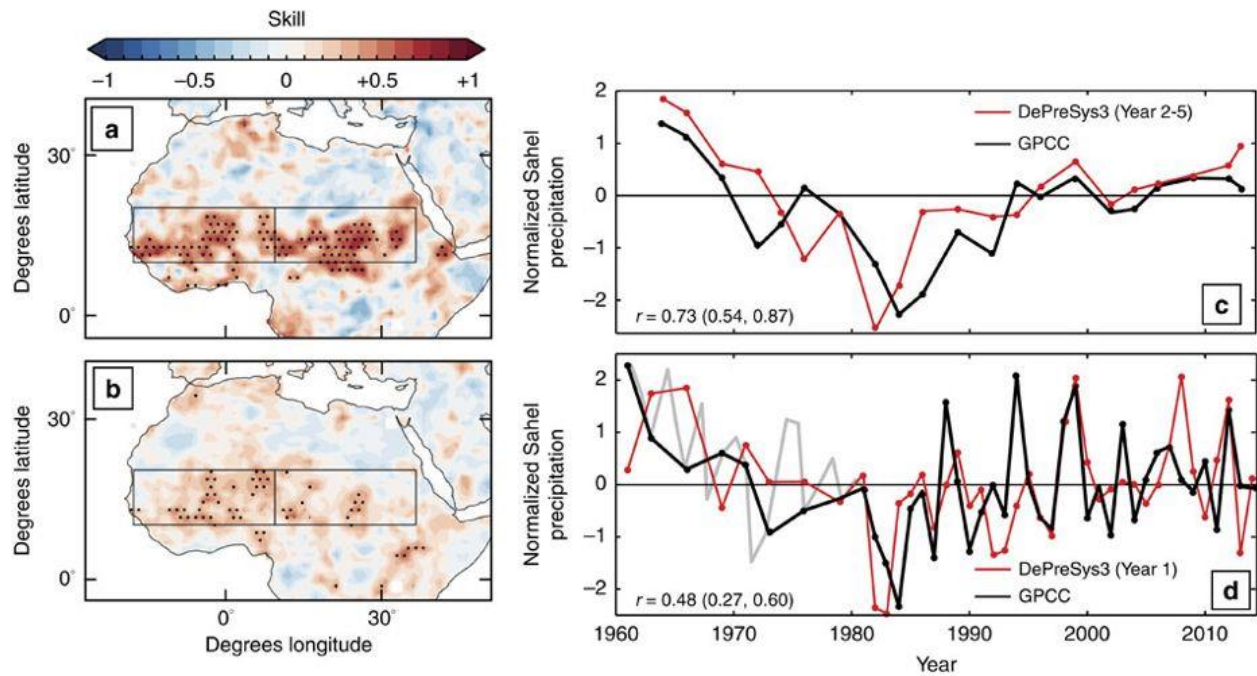
1780  
1781

1782 **Fig. 2.** Forecast probabilities of 13 SSW that occurred on the indicated dates as a function of lead time,

1783 based on ensemble hindcasts from the ECMWF monthly forecasting system. Most of the SSWs are

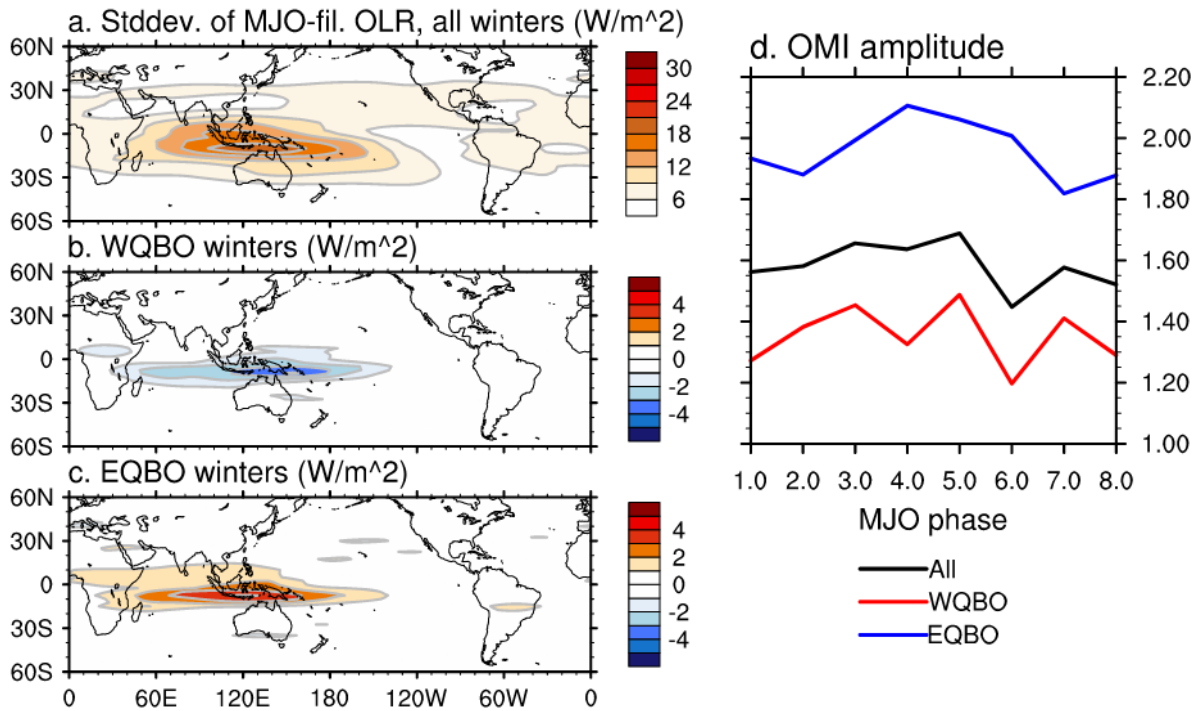
1784 predicted between 8 and 12 days lead time with a probability of 0.5–0.9, which is considerably larger

1785 than the average frequency of SSW occurrence. (From Karpechko 2018.)



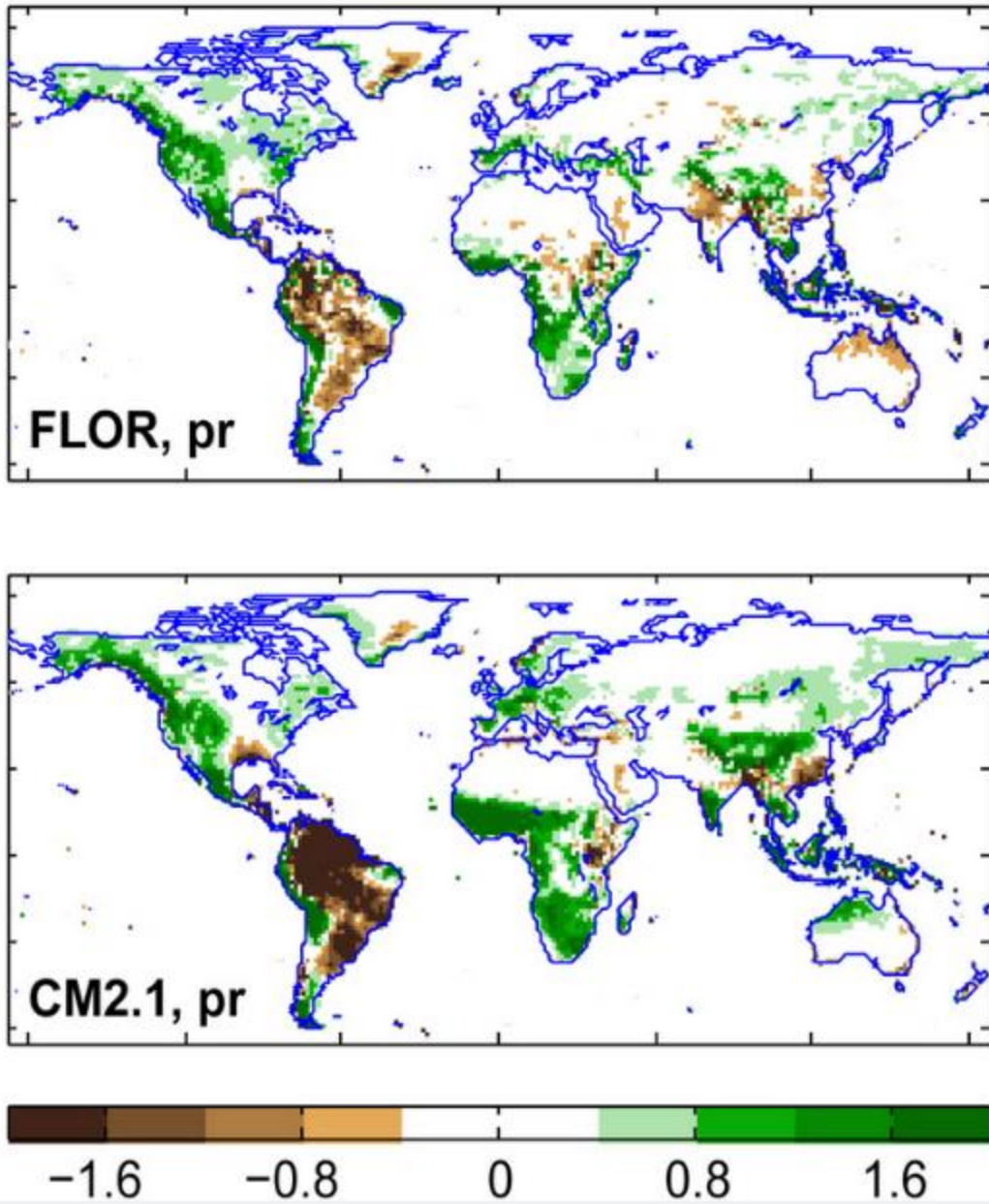
1786  
1787

1788 **Fig. 3.** Skill for predicting linearly detrended Sahel summer rainfall in years 2-5 (upper panels) and year 1  
 1789 (lower panels) in DePreSys hindcasts. Panels (a)-(b) show spatial distributions of anomaly correlation  
 1790 coefficients with stippling indicating 95% significance. Panels (c)-(d) show time series of normalized  
 1791 predicted and GPCCC observed rainfall anomalies in the Sahel region outlined by the boxes in the maps,  
 1792 with correlations and their 5–95% confidence intervals indicated. (From Sheen et al. 2017.)



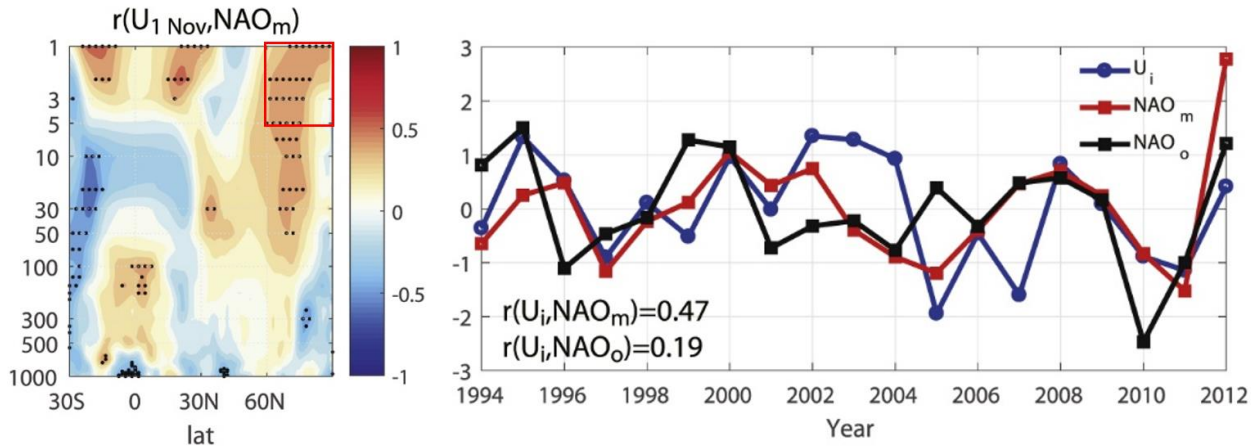
1793  
1794

1795 **Fig. 4.** Influence of QBO phase on MJO amplitude. (a) Standard deviation of wintertime outgoing  
1796 longwave radiation (OLR), filtered to retain temporal and spatial scales characteristic of the MJO, for all  
1797 winters in 1979 to 2012. Differences from these values in winters characterized by QBO westerly  
1798 (WQBO) and easterly (EQBO) phases are shown (b) and (c) respectively. (d) Amplitude of an OLR-based  
1799 MJO index (OMI) as a function of MJO phase for WQBO, EQBO and all winters. (From Yoo and Son 2016.)



1800  
1801

1802 **Fig. 5.** Impact of resolution on precipitation biases in GFDL seasonal prediction models. Atmospheric  
 1803 resolution is approximately 50 km with 32 levels in FLOR (upper panel), and approximately 200 km with  
 1804 24 levels in CM2.1 (lower panel), whereas ocean resolution is approximately 100 km in both models.  
 1805 Higher atmospheric resolution in FLOR reduces precipitation biases in numerous regions including much  
 1806 of the tropics. Annual mean biases over land in  $\text{mm day}^{-1}$  based on 1981-2010 CMAP observations are  
 1807 shown. (After Jia et al. 2015.)



1808

1809 **Fig. 6** Connection between stratospheric initial conditions and predicted winter NAO for UK Met Office

1810 GloSea5 predictions initialized 1 November 1995-2012. Left: correlation between initial zonal wind

1811 anomaly on 1 November and ensemble mean model-predicted surface NAO index ( $NAO_m$ ) during DJF.

1812 Black dots represent values significant at  $\alpha = 0.05$  confidence based on one-tailed test, and mean values

1813 within the red box define an index  $U_i$ . Right: Annual standardized  $U_i$  (blue),  $NAO_m$  (red) and observed

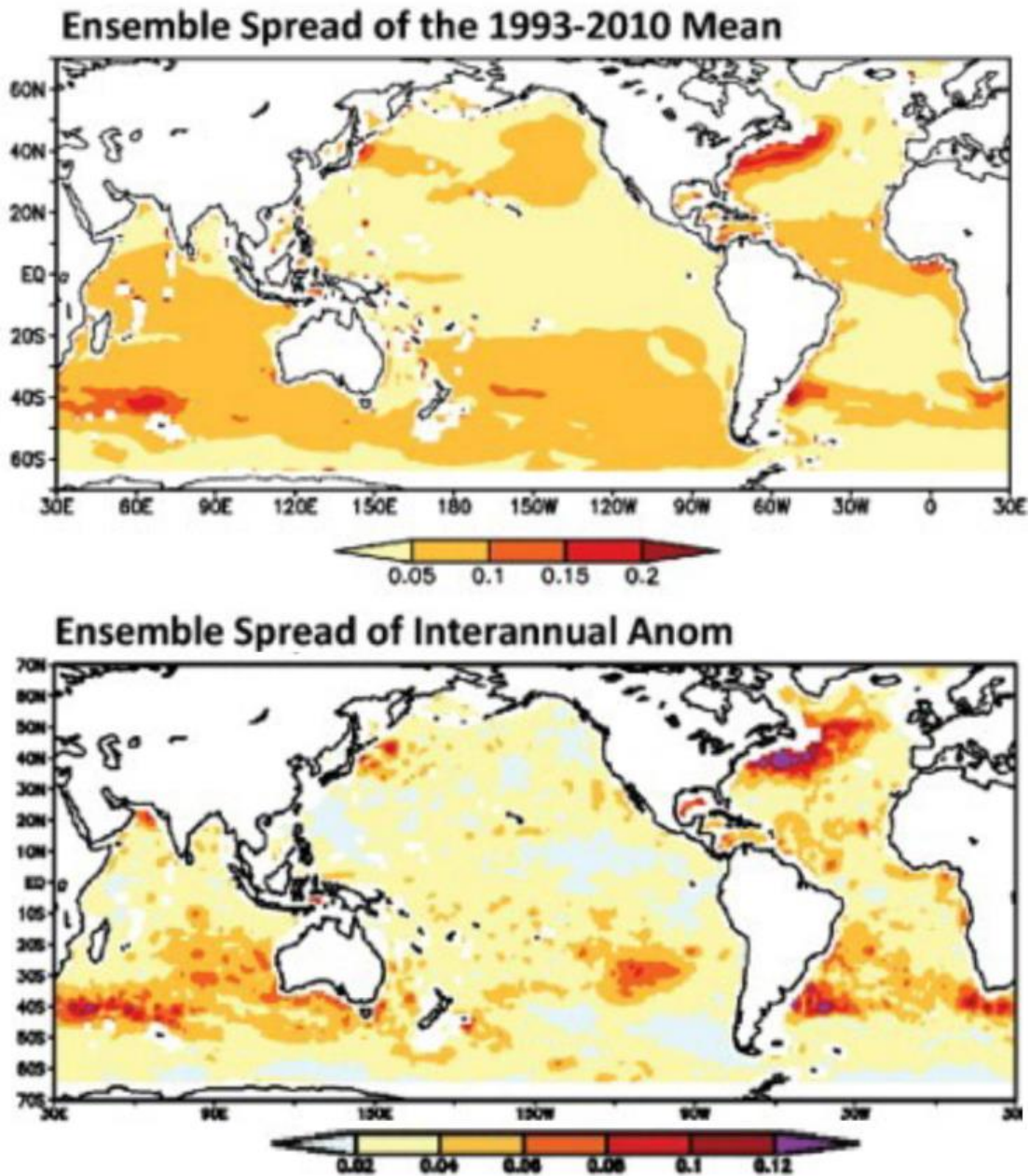
1814 surface NAO index,  $NAO_o$  (black). The correlation of  $U_i$  with  $NAO_m$ , indicated at lower left, is significant at

1815  $\alpha = 0.05$  confidence whereas the lower correlation of  $U_i$  with  $NAO_o$  is not unexpected based on signal to

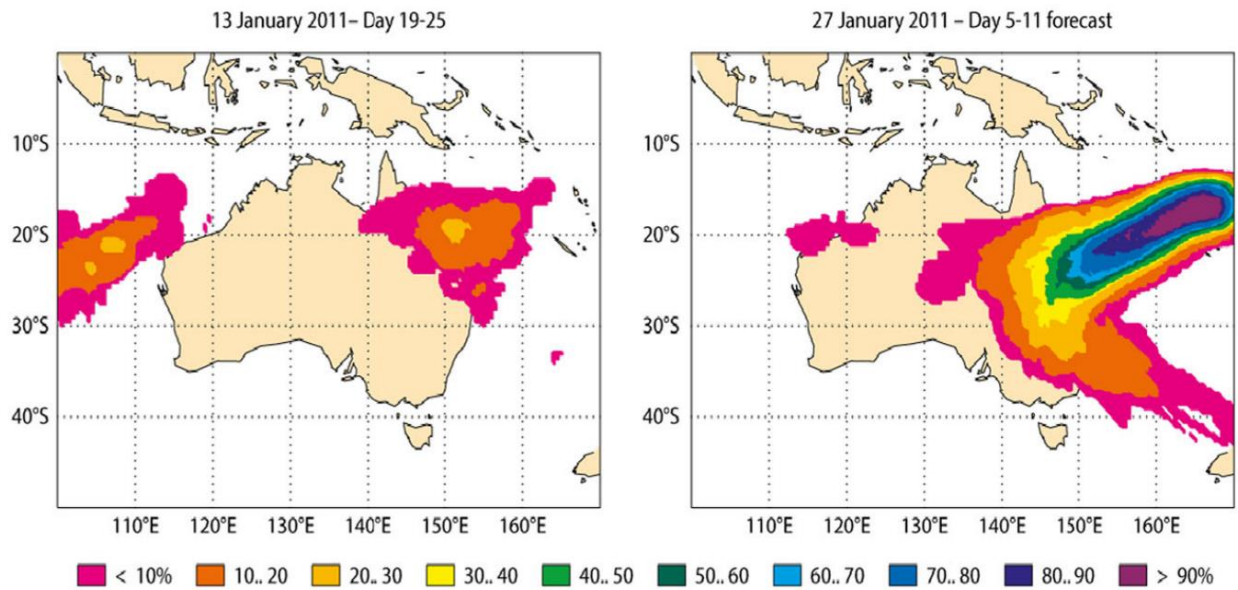
1816 noise considerations and that there is only one realization of observations. The larger correlation of

1817 predicted and observed winter NAO values  $r(NAO_m, NAO_o)=0.62$  suggests that additional sources of

1818 predictability exist. (After Nie et al. 2019.)



1819  
 1820 **Fig. 7.** Consistency across an ensemble of ocean state estimates of depth-averaged salinity over 0–  
 1821 700m, from the Ocean Reanalyses Intercomparison Project. Ensemble standard deviations in both the  
 1822 1993-2010 means (upper panel) and interannually varying monthly anomalies (lower panel) tend to be  
 1823 largest in eddy active regions such as the Gulf Stream, and less well-observed regions such as the  
 1824 Southern Ocean. These differences across state estimates are reflective of uncertainties in ocean initial  
 1825 conditions. (After Balmaseda et al. 2015.)



1826

1827 **Fig. 8.** Elevated probabilities of tropical cyclone occurrence during 31 January to 6 February 2011, based  
 1828 on ECMWF ensemble forecasts forecast starting 13 January with 18 day lead time (left), and 27 January  
 1829 with 4 day lead time (right). Destructive Cyclone Yasi made landfall in northeastern Australia on 3  
 1830 February 2011 as a destructive category 5 storm. (Adapted from Vitart and Robertson 2018).

1831

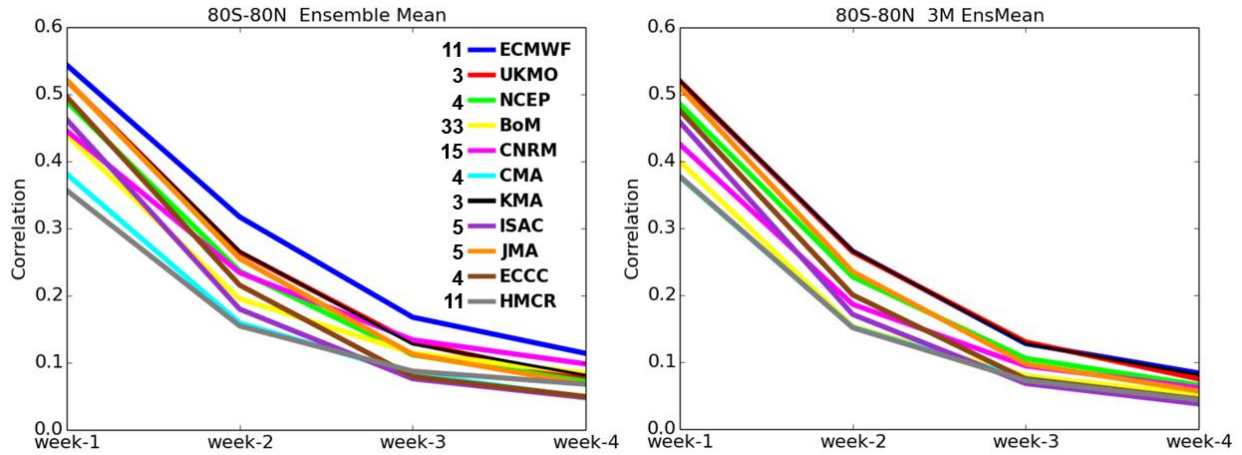
1832

1833

1834

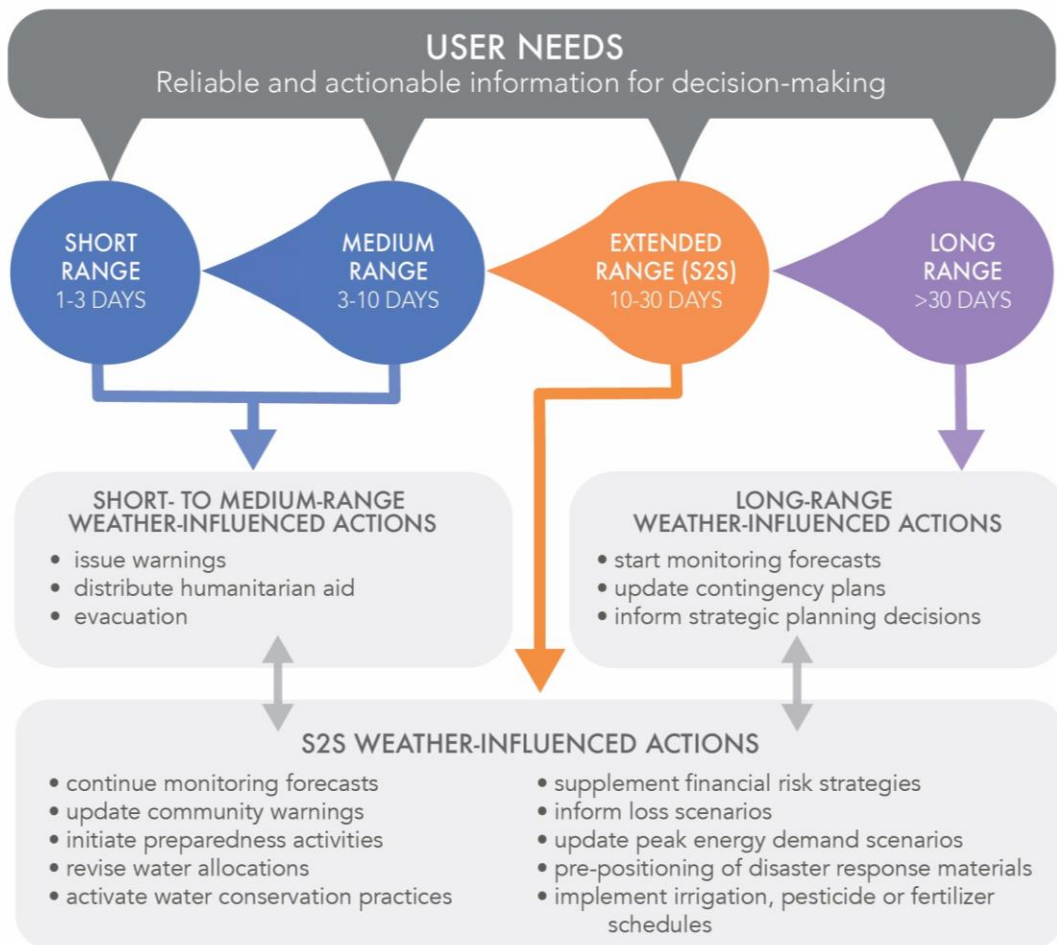
1835



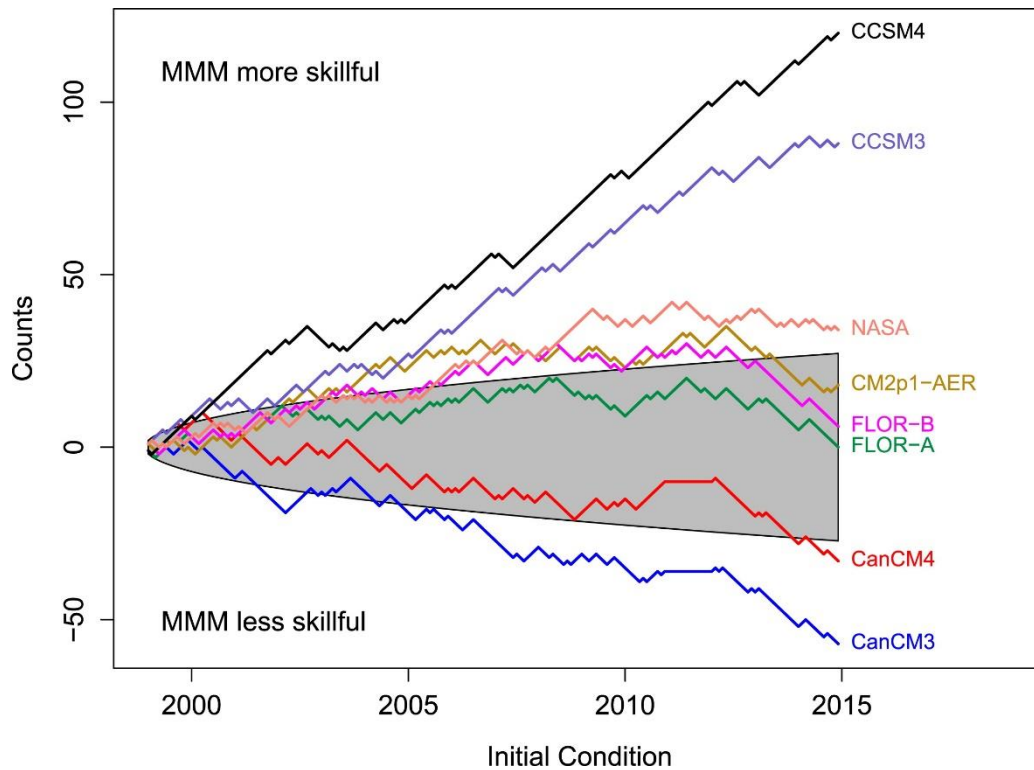


1836  
1837

1838 **Fig. 9.** Global averages of correlations between hindcast and observed precipitation anomalies over the  
 1839 80°S to 80°N latitudinal band for weeks 1-4 for S2S project models initialized from November to March,  
 1840 1999–2009. Left: Hindcast quality assessment based on ensemble means using the full ensemble size for  
 1841 each model, as indicated in the figure legend. Right: Hindcast quality assessment based on ensemble  
 1842 means using three ensemble members for each model. The reduced spread of the lines shown in the  
 1843 right panel when ensemble sizes are identical compared to the spread of the lines shown in the left  
 1844 panel demonstrates the value of the use of larger ensembles for subseasonal precipitation forecasting.  
 1845 (Adapted from de Andrade et al. 2019.)

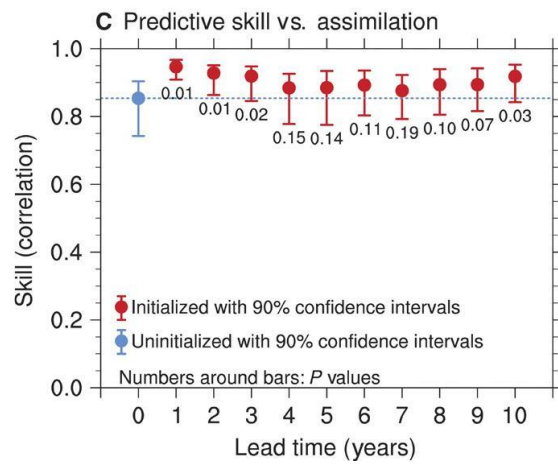
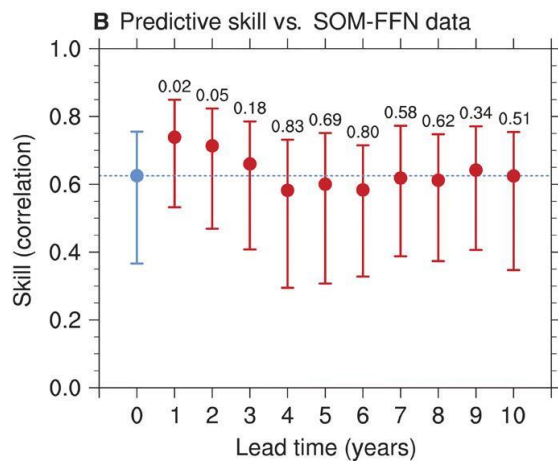
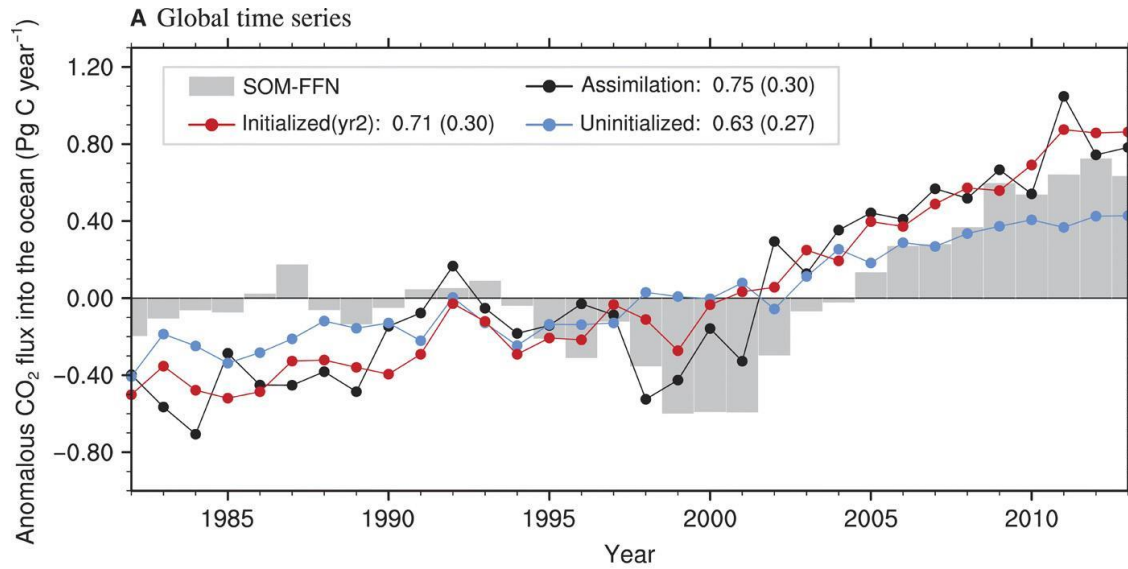


1846  
 1847 **Fig. 10.** Schematic illustration of relationships between a S2S forecast range of 10-30 days and other  
 1848 prediction timescales, including examples of actionable information that can enable decision making by  
 1849 various sectors. Indicated actions are examples that are not exclusive to a particular forecast range.  
 1850 (After White et al. 2017.)



1851  
1852

1853 **Fig. SB1.** Random walk test comparing monthly mean forecasts of the Niño 3.4 index for equatorial  
 1854 Pacific SST at 2.5-month lead, between the multi-model mean (MMM) and individual models in the  
 1855 NMME. Counts (vertical axis) increase by 1 when MMM squared error is smaller than that an individual  
 1856 model (MMM more accurate) and decrease by 1 otherwise (individual model more accurate), and are  
 1857 accumulated forward for all initial months and years (horizontal axis). Accumulated counts above or  
 1858 below the shaded region indicate skill differences according to the squared error metric that are  
 1859 significant with >95% confidence (MMM more skillful above the shaded region and individual model  
 1860 more skillful below). Niño 3.4 anomalies are relative to 1982–98 climatological values, and span each  
 1861 month in 1999-2015. (From DelSole and Tippett 2016.)



1862  
1863  
1864  
1865  
1866  
1867  
1868  
1869  
1870  
1871  
1872

**Fig. SB2.** Temporal evolution and predictive skill of global CO<sub>2</sub> flux into the ocean from the MPI-ESM-HR decadal prediction system. (A) Annual values of anomalous CO<sub>2</sub> flux into the ocean from data-based estimates (SOM-FFN; gray) and MPI-ESM uninitialized simulations (blue), year 2 of initialized decadal predictions (red) and data-constrained assimilation run (black). Anomaly correlations and root-mean-square errors (in parentheses) verifying against SOM-FFN data are indicated. (B) Anomaly correlation skill for global CO<sub>2</sub> flux into the ocean, verifying against SOM-FFN. The blue dot and dashed line show the uninitialized skill for which lead time is not relevant, and the red dots initialized skill for different forecast years, with 90% confidence intervals and P values based on a bootstrap approach indicated. (C) Like (B), but verifying against the assimilation run. (After Li et al. 2019.)